運輸省港湾技術研究所

港湾技術研究所報告

REPORT OF
THE PORT AND HARBOUR RESEARCH INSTITUTE
MINISTRY OF TRANSPORT

VOL. 11 NO. 4 DEC. 1972

NAGASE, YOKOSUKA, JAPAN

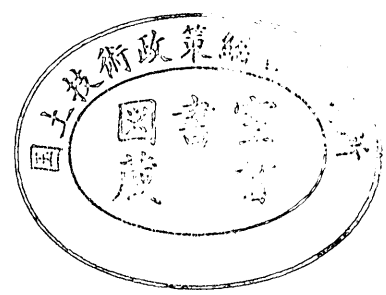

港湾技術研究所報告 (REPORT OF P.H.R.I.)

第11巻 第4号 (Vol. 11, No. 4), 1972年12月 (Dec. 1972)

目 次 (CONTENTS)

REPORT OF THE PORT &
HARBOUR RESEARCH INSTITUTE
Vol. 11 No. 4 (Dec. 1972)

1. Vibratory Response of Laterally Constrained Soils Subjected to A Longitudinal Vibration

Yasufumi UMEHARA*

Synopsis

Laboratory tests, using the resonant column method, were conducted to evaluate the dynamic properties of compacted silty clay under one dimensional condition. The variables considered were the initially applied static load, the vibration amplitude, the water content and the height-diameter ratio.

The water content was found to affect appreciably the values of wave velocity and constrained modulus, but its influence on the damping ratio was small. Although the effect of stress conditions on the dynamic properties of soils was less significant compared with that of water content, the trend toward the S shaped stress strain characteristics was observed.

Wave velocities or constrained moduli could be uniquely determined independently of height-diameter ratio, while the dissipative parameters are dependent on the height-diameter ratio. From this observation, the validity of the assumed mechanical model was discussed.

* Chief of Soil Investigations Section, Soil Division

港湾技術研究所報告
第11巻 第4号 (1972.12)

1. 縦振動を受ける側方拘束粘土の応答特性

梅原靖文*

要　旨

地盤および地盤構造物系の地震動あるいは衝げき荷重等に対する応答解析法の著じるしい進展にともない，入力としての土の常数の基本的性質の解明が望まれる。

本報告では，共振円柱法を用いて，締め固められたシルト質粘土の縦振動応答特性が求められ，それに及ぼす静的応力レベル，振動応力レベル，含水比ならびに供試体の高さと直径の比の影響が調べられた。その結果，次の事実が明らかにされた。

側方変位を拘束した場合の応力波の伝播速度あるいは弾性係数は含水比により大きな影響を受けるが，減衰常数は含水比の相異にあまり影響されない。応力条件の影響は可変範囲が小さいこともあり，含水比による影響ほど著じるしくはないが，求められた弾性係数の傾向からS型の応力ひずみ特性の存在が示唆された。又粘弾性係数に及ぼす高さ直径比の影響を吟味することにより通常使用される粘弾性モデルの妥当性が調べられた。

* 土質部，土質試験課長

CONTENTS

1. Introduction

The behavior and stability of a structure resting on or in the subsoil under a dynamically loaded condition due to earthquake, blasting or vibratory machines have been investigated as a soil-structure dynamic interaction problem. Such a mechanical model as one degree of freedom system, two degree of freedom system or lumped mass system is employed as a useful tool to analyse the responses of soil-structure system to dynamic external forces. Prediction of the actual behavior of the soil-structure system can be successfully performed by adopting proper parameters for soil properties. Although the introduction of the FEM techniques into the stress analysis of the ground made it possible to take into account the real characteristics of the stress-strain relation of a soil more reasonably, the accuracy of the solutions greatly depends on the selection of the soil properties.

These significant advances made in the analysis of problems involving the dynamic loading of soils require to evaluate the pertinent soil properties, usually in the form of Young's moduli, shear moduli or dissipative parameters for a practical purpose, although it is quite questionable in a rigorous sense to represent the stress-strain characteristics of real soils in term of such simple parameters because soils are in general non-elastic, non-linear and non-isotropic. Some of these values may be evaluated from the static test using a triaxial testing apparatus. It has been recognized, however, that the dynamic moduli differ, to a great extent, from those involved in static tests because of strain rate effect, repetition effect, etc. so that the moduli obtained from dynamic tests must be used for the dynamic problems. For this reason, various testing methods as described later have been proposed together with procedures for interpretation of the experimental data.

In representing the stress strain relation by simple parameters, a strain dependency is one of major reasons for discrepancy of real soils from ideal characteristics of stress-strain relation. Some previous workers have tried to express pertinent soil properties, mainly shear moduli by a function of strain level for practical purposes. In this approach, critical soil properties are important and must be evaluated by some laboratory test. Resonant column tests can be considered to be one of the best procedures to evaluate the pertinent soil properties in the range of small strain.

For many problems on earthquake, shear stress-strain relation has been of a major interest, because the ground motions are due primarily to the upward propogation of shear waves from an underlying rock formation. Although compressive stress-strain relation is of a secondary interest in this idealized earthquake, it will give some useful information on the dynamic behavior of soils in some cases. For example, the aseismic design for subaqueous tunnels requires to evaluate the Young's moduli as well as shear moduli. Apart from the earthquake problems, soil properties obtained in longitudinal vibration will give some information on stress analysis in subgrades and base courses for runways subjected to shock loading, and on the effect of vibration generating during the performance of vibro-floatation method on the structures located at the construction site.

Young's moduli of soils subjected to dynamic forces are quite difficult, however, to be evaluated directly in the laboratory test because of lateral inertia effect associated with Poisson's ratio. Instead, constrained moduli can be directly evaluated by laboratory tests, provided the pure one dimensional condition can be satisfactrily simulated.

In this report, vibratory responses of the soil specimen constrained one dimension-

ally to a longitudinal vibration were investigated, from which the pertinent parameters for assumed mechanical model were computed. The effects of variables on these values were investigated and validity of the assumed mechanical model was discussed using the secondary data.

2. Previous studies on determination of dynamic properties of soils

2.1 Generals

A large number of theoretical approaches to the problem of stress wave propagation in solids have been developed on the basis of the knowledge of elasticity or viscoelasticity, with essentially no experimental data to evaluate these theories. These were originally concerned with the studies of ground motion during earthquake and later involved the problems of shock induced stress wave propagation caused by other sources of disturbance like blasting. Subsequent efforts were to evaluate the physical constants such as elastic moduli, viscosity or Poisson's ratio required for predicting the wave propagation phenomena in soil media or vibration characteristics of the subsoil. The available data include tests conducted on both sand and clay with a variety of confining conditions varying from no lateral restraint to one-dimensional condition.

The experimental methods which have been used to determine the dynamic elastic constants of soils may be divided into two general categories: those in which tests are performed on a small sample of soils in laboratory and those in which tests are performed in-situ or in simulated in-situ conditions. The former consists of the following four types: free vibration method, resonant column method, wave propagation method and direct measurement of stress strain relationship. The latter consists of the following four types: seismic method (wave propagation method), elastic-half space method, vibration table method and shock tube method.

2.2 Determination of dynamic properties of soils by laboratory testing

(1) Free vibration method

In this method, the mechanical behavior of the soil sample is defined by the natural period and logarithmic decrement of free vibration, which are generated by shutting the driving power after setting a soil sample in a steady-state vibration, or applying an impulsive force to a soil sample. Since the experimental technique for this type of measurement is simple, this method is widely used for investigation of internal friction of various solids including soil, especially suitable to perform tests on a solid with low internal friction at relatively low frequencies.

Graft-Johnson[1] adopted this technique to measure the damping capacity and elastic modulus of compacted Kaolinite. The impulsive force was applied to the specimen of 1.4 inch in diameter and 3.5 inch long by dropping the rigid mass onto the specimen. The specific damping capacity was calculated from the logarithmic decrement obtained from the decay curves for load and deflection. The elastic modulus was also computed by using the expression for free longitudinal vibrations of a viscoelastic bar which is fixed at an end and has a concentrated mass on the free end.

Hall and Richart[2] used the vibration decay method to evaluate the effects of compression, amplitude of vibration, degree of saturation and grain characteristics on the numerical values of internal damping for four granular soil specimens of 1.59 inch in diameter and 10.8 inch long. The measurements for damping were made by driving the specimen at the resonant frequency of the first mode of vibration then cutting off the power and recording the decay with an oscilloscope camera. Corrections to compensate for the added mass of the pick-up and driver were made in evaluating the

logarithmic decrement from the decay curves.

(2) Resonant column method

The principle of this method is based on the fact that if an oscillating force, whose amplitude is fixed but whose frequency can be varied, is applied to a mechanical system, the amplitude of the resulting vibration becomes maximum at the resonant frequency of the system. The value of the resonant frequency may be related to elastic properties, while the shape of the resonant curve gives a measure of the dissipative force.

Iida and Ishimoto[3, 4] are among the earliest workers who applied this method to investigate the dynamic elastic properties of soils. The rectangular soil specimens of 4×5 cm in cross section and 20 to 40 cm in initial height, which were placed upright on the vibrating plate, were subjected to longitudinal steady-state vibrations or tortional steady-state vibrations, where no lateral confinement was applied to the specimens. The resonant curves were obtained on the basis of the ratio between the amplitude of displacement on the top of the specimen and that of the vibrating plate. The modulus of elasticity, E, and modulus of rigidity, G, were determined from the fundamental resonant frequencies corresponding to both types of vibration. Further, the Poisson's ratio was also computed from the known relation between elastic constants.

Hardin and Richart[5] made an extensive study on the longitudinal and shear wave velocities in granular soils such as Ottawa sand, crushed quartz sand, and crushed quartz silt using the resonant column technique. The variables considered were the confining pressure, the moisture content, void ratio, and grain characteristics of the materials.

Hardin and Black[6] developed a tortional vibration apparatus which made it possible to measure the shear modulus while independently controlling the axial load and confining pressure on a cylindrical specimen of 3.5 cm in diameter and 8 cm long. The specimen was subjected to various static states of stress and then excited into tortional vibration with the base of the specimen fixed and maximum amplitude of vibration at the top. The excitation frequency was varied to obtain resonance as measured by an accelerometer at the top of the specimen.

(3) Wave propagation method

In this method, velocities of elastic waves propagating through solid media are directly measured. The propagation velocities of elastic waves depend on elastic constants and density of the solid, so that the elastic constants can be determined from propagation velocities. If the solid is not perfectly elastic, some of the energy of the stress waves is dissipated as it passes through the medium. The magnitude of this attenuation may be correlated with the internal friction. Main advantages of this method are that a single specimen can be used to cover a wide range of frequencies, and that it is suitable to measure the internal friction because of less energy losses at supports. On the other hand, the disadvantages of this method are that it is not always easy to ensure that a particular type of wave is being generated, and that the interpretation of the results obtained with pulses is often difficult, especially in dispersive media.

Lawrence, quoted by Whitman[7], used the ultrasonic waves to investigate the wave propagation velocity through sand. The sand specimen was confined by a metal ring and some initial axial stress was applied through lucite end caps. The voltage outputs of the two barium titanate crystal were displayed on an osilloscope, and the propagation velocity was computed from the time lapse between the onset of the sent and received signals.

(4) Direct observation of stress-strain curves

The elastic constants and the internal friction could be obtained by making direct measurements of stress and strain during the deformation process of the specimen. By this method, the mechanical behaviour for a given stress cycle can be obtained without making any assumption on the behavior of the specimen. At high rates of loading, however, the experimental determination of the stress-strain relation involves considerable difficulties, because of increasing inertia effect in the measuring apparatus and specimen. The inertia of the specimen results in a non-uniform distribution of stress along its length.

Some techniques to overcome the problems involved in stress strain measurements are described by Kolsky[8]. In order to avoid the non-uniform distribution of stress, the length of the specimen has to be sufficiently short compared with the length of the pulse so that the difference in pressures on both ends can be neglected. However, the treatment of radial motion will still remain as another problem.

Kondner[9] performed the vibratory uniaxial compression tests on the compacted plastic clay specimen of 3 inch long and 1.5 inch in diameter. The dynamic forces and the amplitude of motion of the upper load platen are measured by means of the dynamometer and a piezoelectric type accelerometer, respectively. They computed the complex modulus and loss tangent at a specified frequency, neglecting the inertia effect of the specimen.

Weismann and Hart[10] used a modified triaxial compression apparatus to determine the hysteresis loop in the stress-strain curve during forced vibration of several granular soil samples. Chord moduli, dissipated energy per cycle, potential energy per cycle were computed from the hysteresis loop, which was recorded by an X-Y recorder.

Taylor and Hughes[11] employed a similar technique to that used by Weismann and Hart to investigate the effects of amplitude and number of repetitions of loading on the dynamic shear moduli and energy dissipation of cohesive soils.

Hatano and Watanabe[12] performed the dynamic triaxial compression test on the cylindrical specimen to obtain the dynamic and static moduli and Poisson's ratio for clay, sand and gravel. They measured the vertical deformation and horizontal deformation, from which the secant moduli, Poisson's ratio and overall volumetric strain were computed. Furthermore, the physical constants for assumed mechanical model were computed.

2.3 Prediction of dynamic elastic properties by tests performed under in-situ or simulated in-situ conditions

Various workers have performed the dynamic tests to investigate dynamic properties of soils or dynamic behaviors of soil masses under in-situ or simulated in-situ conditions. The testing methods adopted include the seismic method, elastic half-space method, tests by a vibration table or shock tube, by which elastic properties including elastic moduli, Poissons's ratio, wave propagation velocities and damping parameters could be predicted directly or indirectly under some assumptions.

In seismic method, which uses the same principle as described in the laboratory wave propagation method, a disturbance is induced at one point and the wave propagation is picked up by a sensing device at another point at some distance away. The disturbance may be a single impulse in which case the time for the waves to reach the sensor is measured directly and the velocities are obtained by dividing distance by time.

An impact on an homogeneous, isotropic and elastic medium generates three primary types of waves, i.e. dilatation, distortion and Rayleigh waves. The techniques

to distinguish these three types of waves are rather difficult as discussed by Duke[13] and Shima[14]. A simple method to measure only the shear wave velocity has been devised and widely used for practical purposes.

Elastic half-space method is based on the theory that the elastic constants of soils can be determined from the measurement of the dynamic response of a footing-soil system. This method was originally developed by Reissner and later extended by Sung[15]. In this theory, a system consisting of an osillator-footing resting on soil is considered to be the system of a rigid plate placed on a semi-infinite, homogeneous, isotropic and elastic medium. Dynamic elastic constants can be estimated by measuring the resonant frequency of the system with known dimensions.

In the vibration table method, the simulated in-situ condition is produced in the box placed on the vibration table which is subjected to the forced vibration. The elastic constants and dissipative parameters may be predicted by measuring the response of simulated in-situ ground to the vibration of the vibration table. By this method, the dynamic elastic properties of the simulated in-situ ground may be investigated, taking the inertia effect into consideration.

Arai, et al.[16], used a vibration table to investigate the characteristics of the sand layer during vibration. A number of accelerometers are placed in the sand layer made in the vibration box of 5 m long, 1.5 m high and 1.5 m wide and acceleration responses of each point in the sand layer to the table acceleration, whose amplitude was kept constant for varied frequencies, were obtained. The modulus of rigidity and damping constants of sand layers under various conditions were predicted by assuming the sand layer to be subjected to shear vibration.

3. Restoration of one dimensional conditions

One dimensional condition is, in most cases, acceptable in laboratory testing since a plane wave propagation is assumed in the transmission of body waves due to the release of energy from an earthquake or blasting. Many previous workers have studied one dimensional wave propagation phenomena to get some insight into three dimensional phenomena. In the experiment under the one dimensional condition, conditions, in the other two dimensions must also be controlled. Strain and pressure in the second and third dimensions are usually controlled, either by maintaining zero strain or constant pressure. The constant lateral pressure can be obtained by encasing the soil in a rubber membrane or tube and applying external pressure or internal vacuum. This type of approach was adopted by Selig[17], and others.

The condition of zero lateral strain may be considered to simulate the actual condition more reasonably as long as one dimensional wave propagation is assumed. Acceptable one dimensional column action may impose the following requirements on the design of the tube confining the soil specimen;

1) high radial stiffness to prevent radial motion of the soil, and
2) low axial stiffness to allow the confined materials to follow the movement of adjacent soil and not to retard the axial motion.

It is quite difficult, however, to find the techniques satisfying the above-mentioned requirements rigorously as recognized by previous workers. As practical alternatives to overcome this difficulty, some ideas have been presented to obtain the one-dimensional condition with no or little lateral strain.

Heierli[18] chose the one dimensional case in an attempt to investigate the fundamental phenomena of inelastic wave propagation. No assumption was made regarding

the stress strain properties of the material or the behaviors of the end boundaries of the soil column. In order to assure the use of the relevant properties for the calculations of wave propagation, the stress-strain relation must be measured under approximately the same condition as will occur in the actual wave propagation. To do this, Heierli performed the dynamic oedometer test on a soil sample. This kind of test will cause another problem of side friction, which prevents the vertical motion of the soil sample and cause the non-uniform distribution of stresses throughout the sample at any given time. To overcome this problem, Heierli used a sample height that was only a small fraction (say, 1/10) of the wave length of the induced pressure.

Stoll and Ebeido[19] investigated the wave propagation phenomena through the granular specimen by means of a shock tube technique. A cylindrical sand column of 12 inch or 24 inch long and 2-5/8 inch in diameter were confined laterally by a container constructed of latex rubber reinforced by a spiral of steel wire. A dynamic stress input was applied by an air impulse from a pneumatic shock tube, and stress gages were imbedded at various positions in the specimen to measure wave velocities and dynamic pressures. They reported that the stress-strain curve was S-shaped, which was the most probable form of stress-strain curve for a constrained granular media, as suggested by Whitman, et al.[7], based on the result of rapid loading tests.

Stoll and Hess[20] have performed the analytical investigation on transient wave phenomena in a circular bar which is subjected to a frictionless elastic restraint on the radial boundary. The theoretical results on a transient state of a bar due to a shock-induced pressure were used to interpret the results from a certain type of experimental configuration, in particular, to assess the effects of radial motion in the experiment. They reported that the radial inertia, warping, and other three dimensional motion result in an oscillation with short period superimposed to the basic wave obtained from the rigorous one dimensional case. Further, they reported that these effects depend on the stiffness of the elastic shell relative to the confined materials, and that a stiffer casing would give results more closely resembling the one dimensional case.

Seaman[21] investigated the wave propagation phenomena in typical near surface soils. Several dynamic tests on small samples of these soils were conducted in a laboratory compression tester. These results were used to develop the theoretical model to predict the wave propagation results. For the wave propagation tests, Seaman's approach was to apply a pulse loading to a one dimensional column of soil. To obtain the one dimensional condition, the soil tube was constructed of alternative rings of aluminum and neoprene rubber. The aluminum rings provided a high radial stiffness to prevent radial motion of the soil and rubber spacers reduced the axial stiffness of the tube, which was made up in segments, each about 0.7 meters long.

As described above, some special shells were used to offer a stiff radial restraint with a minimum of tangential traction, resulting in motions that are predominant in the axial direction. This type of restraint was obtained by constructing the shell of discrete rings or in the form of a helix with the rings or loops separated by a small spacing.

It is rather difficult, however, to confirm whether or not the perfect, if possible, or approximately perfect one dimensional motion can be produced by a technique to restrain the radial motion of the specimen. A rigid casing can be used for a short specimen, since a side friction effect may be considered negligible. In this case, as assumed in the method of determining the dynamic properties by the direct measurement of stress-strain relation, the assumption of the uniform distribution of stresses

through the specimen may be valid, because no wave propagation takes place. In case of a resonant column method, the wave propagation effect in a steady-state vibration may be used for determination of dynamic properties, in which a longer specimen is desirable to make the wave propagation effect eminent. Since the use of a rigid casing causes a more serious side friction effect, an alternative method must be used to restrain the radial motion while reducing the side friction effect.

In Seaman's method, these two requirements seem to be satisfied. As for the radial stiffness of the casing to simulate a zero radial strain condition, the radial strain was only 100 micro strain with an axial pressure of 102 psi, whlist the axial stiffness of the casing was about 816 psi and was so small that the casing absorved less than 1 persent of the total applied force.

4. Mechanical representation of dynamic behaviours of soils subjected to a vibratory loading

Soils are neither ideally elastic nor ideally plastic, and have a very complicated nature, which can not be explained rigorously by already established mechanical models such as the Hookian, Maxwell and Kelvin models. Ideally, a general constitutive relationship, to describe both the static and dynamic response of soils, should be based on a rational physical system. When this approach is attempted, however, formidable difficulties will take place. As a practical alternative, it is necessary to rely on a soil model partly based on the physical nature of soil structure and partly based on the observed phenomenological response.

From the phenomenological point of view, it is well known that the soils show visco-elastic behaviours, which may be represented by some combinations of spring and dash pot. Among them three types of models are often used, which are the Maxwell, Kelvin and Maxwell-Kelvin models. The simplest model is the Maxwell model composed of spring and dash pot in series. The Kelvin model consists of spring and dash pot in parallel, while the Maxwell-Kelvin model consists of a spring and Kelvin model in series. The behaviours of these visco-elastic solids and the characteristics of wave propagation through these solids are discussed in detail by Kolsky[8].

To analyse the dynamic phenomena of laterally restrained soil specimen subjected to a vibratory loading, the simple Kelvin model has been chosen as the first approximation as adopted by Yong, et al.[22]. This approach was also adopted by those who investigated the ratios of input and output displacements of unconfined soil specimens. In the present study, on the other hand, ratios of input and output stresses are investigated on laterally constrained soil specimens.

To establish the basic relations for analysing the vibratory response of the soil specimen, let it be assumed that each plane cross-section of the rod consisting of a laterally restrained soil specimen remains plane during the motion, and that the stress over it is uniform. The rod is assumed to be composed of visco-elastic solids represented by the Kelvin model, whose stress-strain relation is indicated in the form:

$$\sigma = E_c \varepsilon + \eta \dot{\varepsilon} \qquad (1)$$

where E_c: constrained modulus
η: coefficient of solid viscosity
ε: strain

The basic equation of motion of the rod for one dimensional vibration will be given in the form:

$$\rho\frac{\partial^2 u}{\partial t^2}=E_c\frac{\partial^2 u}{\partial x^2}+\eta\frac{\partial^3 u}{\partial x^2\partial t} \tag{2}$$

The initial and boundary conditions for free vibrations are given in the form:

$$\begin{aligned} &u(x,\ 0)=0\\ &u(0,\ t)=0\\ &\frac{\partial u}{\partial x}=0 \text{ at } x=H \end{aligned} \tag{3}$$

The boundary conditions for steady state forced vibrations can be given by

$$\begin{aligned} &u(0,\ t)=0\\ &\sigma(H,\ t)=Ce^{ipt} \end{aligned} \tag{4}$$

where C is an amplitude of input stress and kept constant during vibration, and p is a circular frequency of forced vibration.

Equation (2) can be solved under the associated initial and boundary conditions by means of either Laplace transform technique or variable separation method. The complete solution is shown in the Appendix. The term of free vibration disappears very rapidly and only the term of steady state forced vibration is left.

The main interest at present is the magnitude of the output stress at the bottom of the specimen caused by the input stress induced at the top of the specimen, especially the ratio between input and output stresses, σ_I and σ_O. These are given as follows:

$$\sigma(0,\ t)=\frac{\sqrt{2}C}{\sqrt{\cos 2f_1H+\cosh 2f_2H}}\cdot\cos(pt+\psi_s) \tag{5}$$

$$\sigma_O/\sigma_I=\frac{\sqrt{2}}{\sqrt{\cos 2f_1H+\cosh 2f_2H}} \tag{6}$$

$$\psi_s=\tan^{-1}(\tan f_1H\tanh f_2H) \tag{7}$$

$$\left.\begin{matrix} f_1H\\ f_2H \end{matrix}\right\}=\frac{\pi/2\cdot(2r-1)}{\left(1+4\left(\frac{p}{n}\right)^2h_r^2\right)^{1/4}}\sqrt{\frac{1}{2}\left(1\pm\frac{1}{\sqrt{1+4(p/n)^2h_r^2}}\right)} \tag{8}$$

where ψ_s: phase difference between input and output stresses

p/n: frequency ratio; p is frequency of forced vibration and n is natural frequency

h_r: damping ratio defined by $h_r=\frac{\pi\eta}{4H\sqrt{\rho E_c}}\cdot(2r-1)(r=1,\ 2,\ 3\cdots\cdots)$ (9)

In the above derivation, the resonant frequency, f_r, is given in the form:

$$f_r=\frac{(2r-1)}{4H}\cdot V_p\cdot\sqrt{1-h_r^2} \tag{10}$$

where V_p is longitudinal wave velocity and defined by

$$V_p=\sqrt{\frac{E_c}{\rho}} \tag{11}$$

The acceleration at the top of the specimen and the phase difference between input stress and resulting acceleration are given respectively,

$$\ddot{u}_{x=H}=\frac{-2C\sqrt{(f_1H)^2+(f_2H)^2}\sqrt{\sin^2 2f_1H+\sinh^2 2f_2H}}{\rho H(\cos 2f_1H+\cosh 2f_2H)}\cdot e^{i(pt+\psi_a)} \tag{12}$$

$$\psi_a=\tan^{-1}\frac{f_1H\sinh 2f_2H\cos 2f_1H-f_2H\sin 2f_1H\cosh 2f_2H}{f_1H\sin 2f_1H\cosh 2f_2H+f_2H\sinh 2f_2H\cos 2f_1H} \tag{13}$$

Expressing Eq. (12) in a non-dimensional form,

$$\frac{\rho H\ddot{u}}{C}=-\frac{2\sqrt{(f_1H)^2+(f_2H)^2}\cdot\sqrt{\sin^2 2f_1H+\sinh^2 2f_2H}}{\cos 2f_1H+\cosh 2f_2H}\cdot e^{i(pt+\psi_a)} \tag{14}$$

The computed theoretical curves for stress response, phase differences, and non-dimensional acceleration (amplitude) are shown in terms of frequency ratio for various values of damping ratio in Figs. 1 and 2.

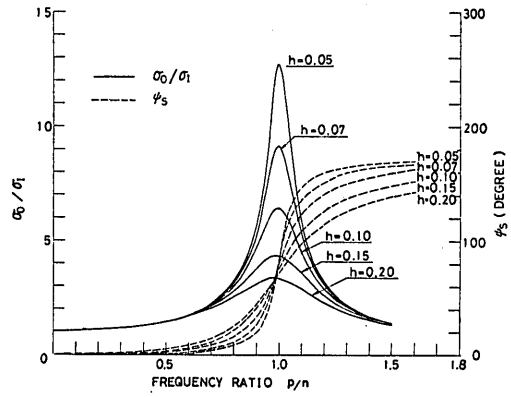

Fig. 1 Theoretical Frequency Response and Phase Differences

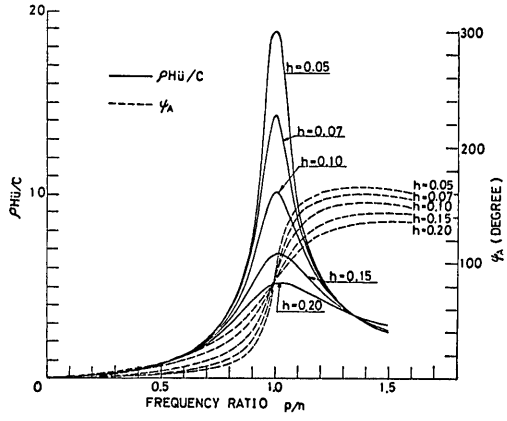

Fig. 2 Non-Dimensional Acceleration and Phase Differences

5. Experiment

5.1 Apparatus

The arrangement of the apparatus used in the present experiment is schematically shown in Fig. 3. The vibrator, weighing 30 lb (13.26 kg), is suspended by two sets of wire and balancing weight. The specimen is restrained with 1/4 in. (0.635 cm) thick

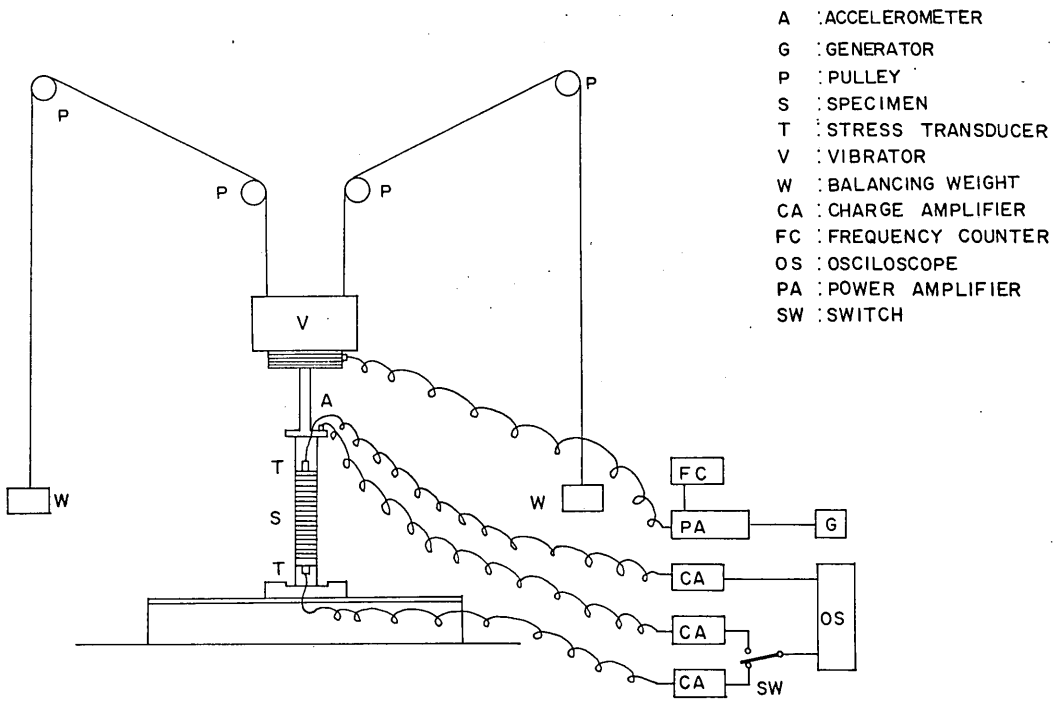

Fig. 3 Schematic Diagram of Arrangement of Experimental Apparatus

aluminum rings. Aluminum top platen is connected to the vibrator with 3 in. (7.62 cm) long steel rod, and aluminum lower platen is fixed on the steel base plate.

(1) Loading apparatus

The static load, which is kept constant during vibration, is applied by adjusting the difference in weight between the vibrator and balancing weight. A vibratory load is given by an electro-magnetic vibration generator having a 25 lb (11.34 kg) force capacity. A frequency generator supplies AC current amplified by a power amplifier to the driving coil attached to the armature of a vibration generator.

(2) Measuring equipments

Input and output stresses are measured with the aid of the Suffield piezo-electric transducers mounted on the top and bottom platens. The piezo-electric transducer responds very quickly to the instantaneous loading and picks up dynamic stresses.

This transducer is calibrated with a Kistler piezo-electric transducer of known calibration. These two transducers are mounted on the bottom of a water tank covered with a thin rubber membrane, to which the sinusoidally vibrating load is applied by the above mentioned electro-magnetic vibration generator. Both transducers mounted on the top and bottom platens are connected to the charge amplifier with low noise cables.

The acceleration at the top of the specimen is measured by an accelerometer attached to the top platen. Calibration of the transducer is also performed by exciting it with a known vibration by the electro-magnetic vibration generator. The accelerometer is also connected to the charge amplifier with a low noise cable.

Kistler transisterised charge amplifiers are used with long input cables for measurement up to 100,000 cps. Six-feet low noise cables from the installed transducer are

used to avoid any noise and the obtained amplified signals are passed on to the oscilloscope through coaxial cables.

5.2 Sample preparation

The sample used for the experiment was a compacted silty clay called Grundite, which is commercially available in an air dry state and has a liquid limit of 65% and a plastic limit of 33%. The grain size distribution is shown in Fig. 4.

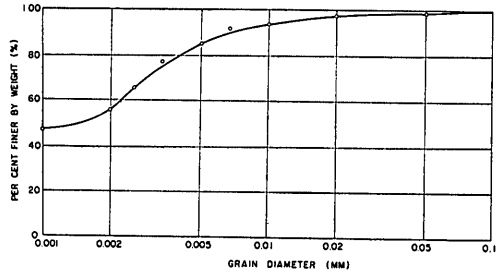

Fig. 4 Grain Size Accumulation Curve

A certain amount of Grundite was mixed with a required amount of water and cured for 24 hours in a vinyl pack. The soil specimen, enclosed with discrete aluminum rings of 1/4 in. high and separated by a pair of split rings of 1/8 in. high, was made by compaction in a specially constructed compaction mold. The specimen was then removed from the mold, weighed together with attachments, and left for 20 hours before testing.

Diameter of cylindrical specimen was D=1.5 in. (3.81 cm), and its height was changed so as to obtain the height-diameter ratio of H/D=2, 4 and 8. Water content of the specimen was found to be in the range of 18% to 40%.

5.3 Experimental technique

The specimen was placed between the upper and lower platens together with necessary attachments. The lower platen was rigidly clamped to the base plate. The upper platen was fixed to the electromagnetic vibration generator, the weight of which being in equilibrium with the balancing weight. Then the upper platen was lowered to the top of the specimen. All pairs of the split rings enclosing the specimen were removed prior to loading so that the cylindrical specimen was to be confined with discrete rings separated by a small spacing as shown in Fig. 5. This technique for confining specimen is similar to that adopted by Seaman[21], which is described in 3. A specified static load was applied by removing a part of the balancing weights.

Application of the static load resulted in the occurrence of transient creep of the specimen. When major part of the creep had been completed, a sinusoidally vibrating stress was induced to the top of the specimen by oscillating the upper platen with the rod fixed to the electro-magnetic vibration generator.

In order to avoid the transient dynamic effect, the measurement of stress and acceleration was started after confirming a steady state of oscillation to have occurred for a sufficiently long period. The measurement was performed of the following items: the double amplitude of induced vibratory stress $\sigma_I(=\sigma_D)$, which was monitored at the top of the specimen; the double amplitude of resulting vibratory stress, σ_O, which was monitored at the bottom of the specimen; the double amplitude of acceleration, α, which was resulted at the top of the specimen for maintanining the specified level of input stress; phase difference between induced and resulted stresses (or input and

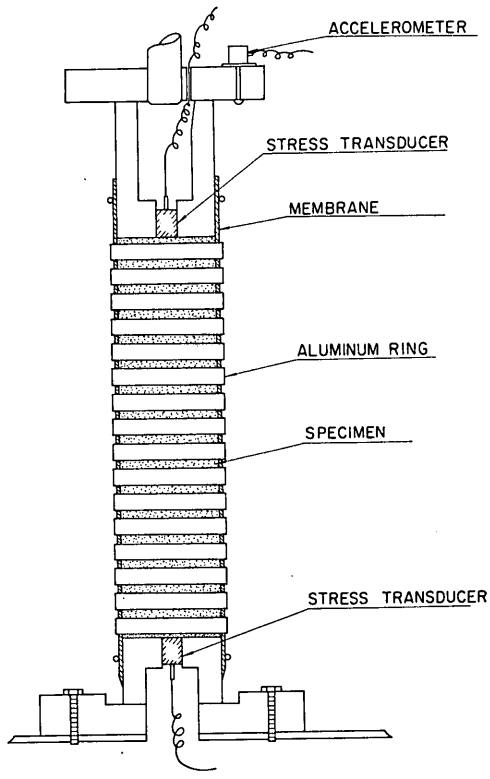

Fig. 5 Specimen Confined with Aluminum Rings

output stresses), ψ_s; phase difference between induced stress and resulted acceleration, ψ_a.

The oscillatory stresses were measured by means of Suffield stress transducers, while the acceleration was measured by a quartz type of accelerometer. These signals were amplified by charge amplifiers and viewed on a dual channel oscilloscope.

In the course of the vibration, an amplitude of the induced vibratory stress was kept constant, and a frequency was varied. As for the stress level, the following combinations of static stress level, σ_S, and dynamic stress level, $\sigma_D(=\sigma_I)$, were chosen.

Static stress level, σ_S	Dynamic stress level, σ_D
0.175 kg/cm^2	0.031 kg/cm^2
0.36 kg/cm^2	0.031 kg/cm^2
0.72 kg/cm^2	0.012, 0.021 and 0.031 kg/cm^2

6. Test results

6.1 Frequency response curves

According to a combination of stress levels, water content and height-diameter ratio of specimen, 76 different cases were examined. In each of them, the stress responses were computed for varying frequencies. Based on these results, the freqency response curves were obtained by assuming a visco-elastic model which has two

visco-elastic parameters. The most reasonable theoretical curve for the experimental data were determined through a curve fitting procedure using a computor program.

In order to see an influence of the testing condition on the relation between stress response and frequency, typical frequency response curves are shown in Figs. 6 through 12.

Fig. 6 shows the variation of frequency response curves with height-diameter ratio H/D for the case where the static and dynamic stress levels are $\sigma_S=0.175\,kg/cm^2$ and $\sigma_D=0.031\,kg/cm^2$ respectively, and water content is about 25%. As seen in the figure, as the height-diameter ratio decreases, frequency response curves become flatter and the resonant frequency increases.

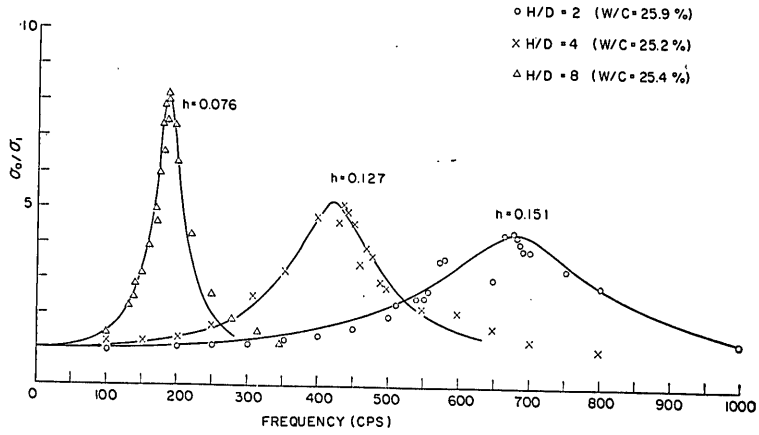

Fig. 6 Frequency Response (Influence of Height-Diameter Ratio)
$\sigma_S=0.175\,kg/cm^2$, $\sigma_D=0.031\,kg/cm^2$

Fig. 7 shows also an influence of the H/D value on the frequency response curve

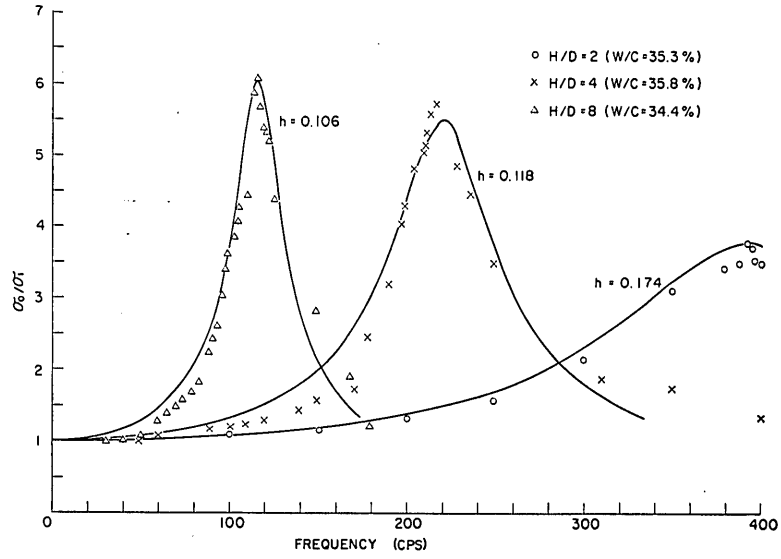

Fig. 7 Frequency Response (Influence of Height-Diameter Ratio)
$\sigma_S=0.36\,kg/cm^2$, $\sigma_D=0.031\,kg/cm^2$

for the case of σ_S=0.175 kg/cm² and σ_D=0.031 kg/cm² and water content of about 35%. Although a manner of variation of the response curves with height-diameter ratio is similar to those shown in Fig. 6, it may be observed in this softer specimen that an agreement of the experimental data with the above mentioned theoretical curves is relatively poor.

Figs. 8 and 9 show the variation of frequency response curves with the static stress level σ_S for the case of water content of 25.4% and 30.9%, where H/D=4 and σ_D=0.031 kg/cm². From these figures, it may be said that the resonant frequency increases as the static load increases. However, the influence of water content on the

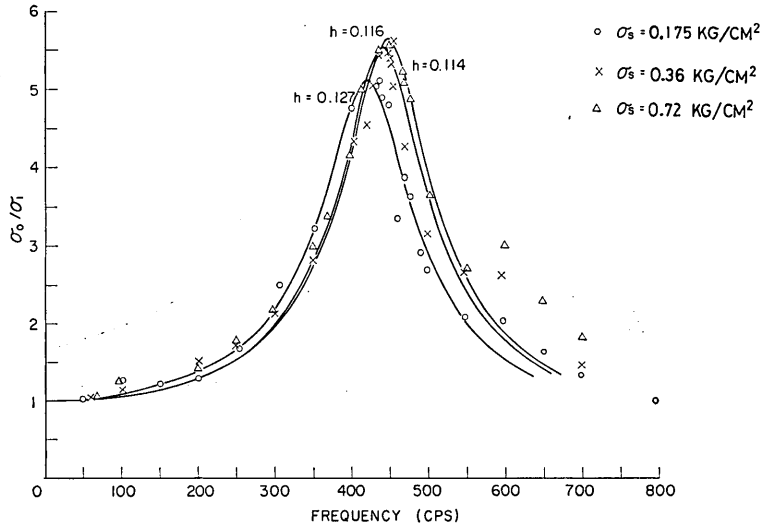

Fig. 8 Frequency Response (Influence of Static Stress)
H/D=4, σ_D=0.031 kg/cm²

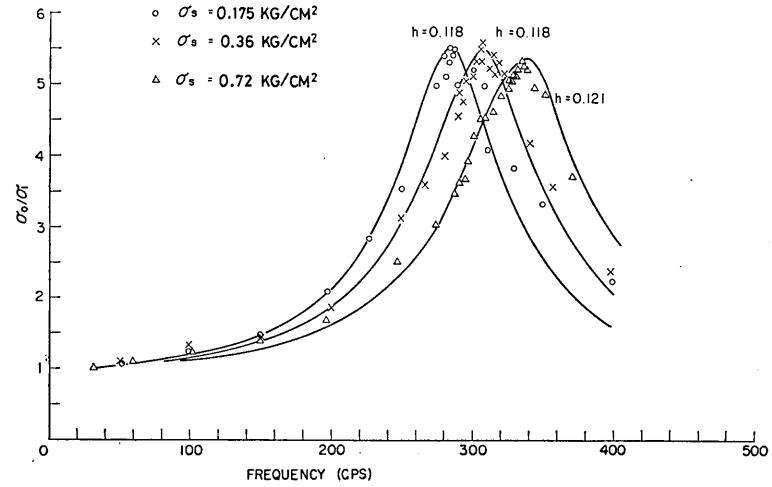

Fig. 9 Frequency Response (Influence of Static Stress)
H/D=4, σ_D=0.031 kg/cm²

peak value of stress ratio are rather complicated. For the case of water content of 25.4%, the higher the static load, the higher the peak value of stress ratio, whilst for the case of water content of 30.9%, vice versa. This fact may suggest that, at some value of water content, the peak value of stress ratio remains essentially unchanged irrespective of a change in static load.

Figs. 10 through 12 show the variation of frequency response curves with water content for the following three cases;

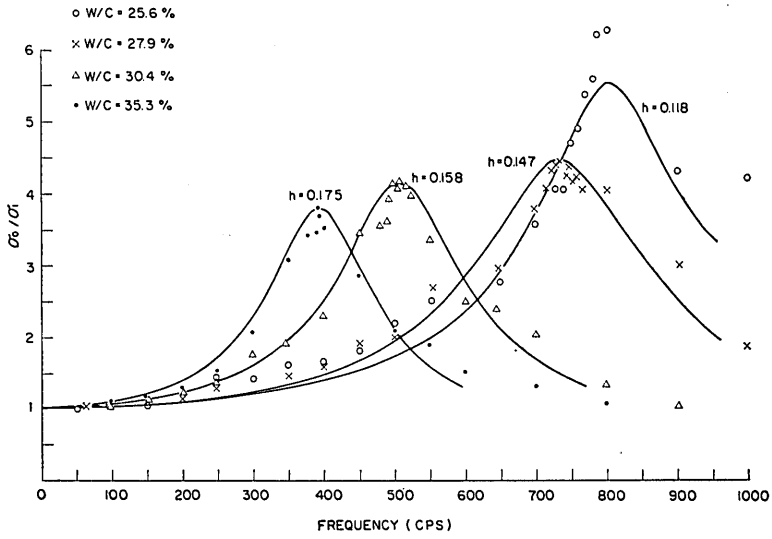

Fig. 10 Frequency Response (Influence of Water Content)
$H/D=2$, $\sigma_S=0.36\ \mathrm{kg/cm^2}$, $\sigma_D=0.031\ \mathrm{kg/cm^2}$

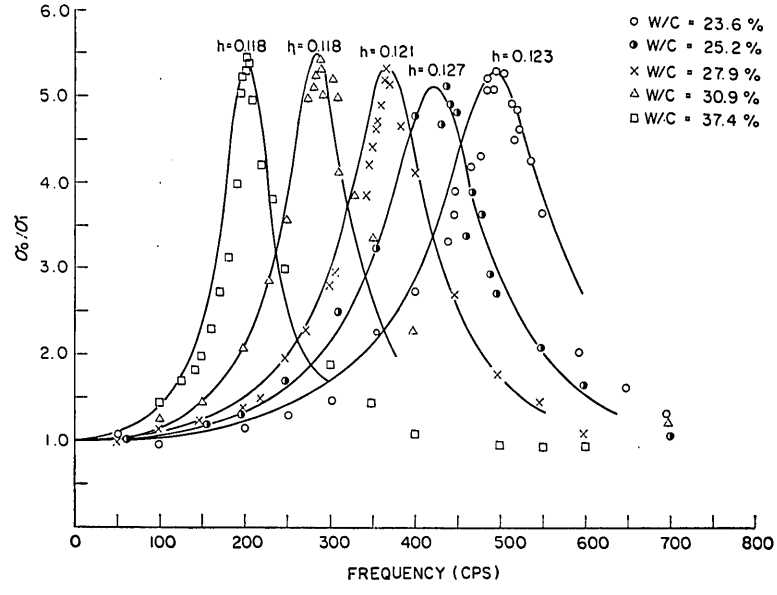

Fig. 11 Frequency Response (Influence of Water Content)
$H/D=4$, $\sigma_S=0.175\ \mathrm{kg/cm^2}$, $\sigma_D=0.031\ \mathrm{kg/cm^2}$

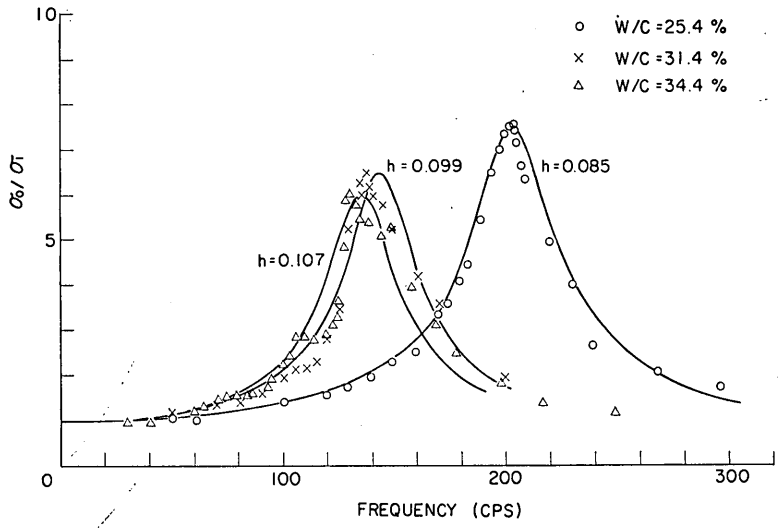

Fig. 12 Frequency Response (Influence of Water Content)
$H/D=8$, $\sigma_S=0.72$ kg/cm², $\sigma_D=0.031$ kg/cm²

	H/D	σ_S	σ_D
1)	2	0.36 kg/cm²	0.031 kg/cm²
2)	4	0.175 〃	0.031 〃
3)	8	0.72 〃	0.031 〃

It can be said from these figures that both the resonant frequency and the peak value of stress ratio decrease as water content increases. It should be noted, however, that, in the case of $H/D=4$, the frequency response curves simply shift to the left without any appreciable change in peak value of stress ratio as water content increases.

The frequency corresponding to the peak value on the frequency response curve is the resonant frequency, which coupled with the shape of the frequency response curve, leads to the determination of mechanical parameters for the assumed model. All results computed are tabulated in Tables 1 and 2. Some factors governing these mechanical parameters are examined mainly in relation to the variation of mechanical parameters with water content in the following sections.

It should be noted that the change in water content leads to the change in density, which affects the wave velocity. Thus it must be examined whether or not a significant difference in density appears among specimens with the same water content, but different height. Fig. 13 shows the relation between dry density and water content for all the specimen used for the present experiment. The solid curve shows the result of standard compaction test made with use of the shortest mold. It may be seen that the dry density is determined solely by the water content irrespective of height-diameter ratio. Explanation to this fact may be that, in the course of compaction in the sample preparation, the density of each has attained the limit value for a given water content so that an additional compaction effort causes no further increase in density.

6.2 Resonant frequency

TABLE - 1 EXPERIMENTAL AND COMPUTED RESULTS

No.	H/D	W/C %	σ_S kg/cm²	σ_D kg/cm²	Fr cps	Accel. g	h	V_p m/sec	Dynamic Elastic Modulus (kg/cm²) constrained	$\nu=0.30$	$\nu=0.35$	$\nu=0.40$	η $\frac{g\cdot sec}{cm^2}$
1	2	25.9	0.175	0.031	682.0	9.12	0.151	227.8	0.997×10^3	0.741×10^3	0.621×10^3	0.465×10^3	69.5
2	2	25.9	0.36	0.031	683.0	—	0.170	228.1	0.100×10^4	0.745×10^3	0.625×10^3	0.468×10^3	78.2
3	2	25.9	0.72	0.012	805.0	1.49	0.118	266.9	0.137×10^4	0.102×10^4	0.855×10^3	0.640×10^3	63.5
4	2	25.9	0.72	0.021	795.0	2.34	0.135	264.1	0.134×10^4	0.978×10^3	0.837×10^3	0.627×10^3	71.7
5	2	25.9	0.72	0.031	781.0	—	0.143	259.4	0.130×10^4	0.964×10^3	0.809×10^3	0.606×10^3	74.9
6	2	25.6	0.175	0.031	721.0	—	0.113	240.3	0.115×10^4	0.856×10^3	0.718×10^3	0.537×10^3	56.9
7	2	25.6	0.36	0.031	805.0	6.22	0.118	267.2	0.143×10^4	0.106×10^4	0.891×10^3	0.668×10^3	66.0
8	2	25.6	0.72	0.031	850.0	—	0.139	282.5	0.160×10^4	0.199×10^4	0.998×10^3	0.747×10^3	82.1
9	2	28.8	0.175	0.031	600.0	8.05	0.130	202.3	0.796×10^3	0.592×10^3	0.496×10^3	0.372×10^3	54.3
10	2	28.8	0.36	0.031	647.0	7.69	0.136	217.3	0.923×10^3	0.686×10^3	0.576×10^3	0.431×10^3	61.2
11	2	28.8	0.72	0.031									
12	2	30.4	0.175	0.031	497.0	6.67	0.125	166.2	0.522×10^3	0.388×10^3	0.325×10^3	0.244×10^3	41.5
13	2	30.4	0.36	0.031	507.0	6.82	0.158	170.1	0.548×10^3	0.407×10^3	0.341×10^3	0.256×10^3	53.5
14	2	30.4	0.72	0.012	575.5	—	0.128	192.0	0.698×10^3	0.519×10^3	0.435×10^3	0.326×10^3	48.9
15	2	30.4	0.72	0.021	625.0	5.22	0.145	208.9	0.828×10^3	0.615×10^3	0.516×10^3	0.386×10^3	60.4
16	2	30.4	0.72	0.031	610.0	7.56	0.158	204.0	0.791×10^3	0.587×10^3	0.493×10^3	0.369×10^3	64.5
17	2	33.0	0.175	0.031	414.0	7.01	0.150	138.9	0.354×10^3	0.263×10^3	0.220×10^3	0.165×10^3	40.2
18	2	33.0	0.36	0.031	435.0	5.60	0.143	145.6	0.389×10^3	0.289×10^3	0.242×10^3	0.182×10^3	40.2
19	2	33.0	0.72	0.012	541.0	—	0.143	180.5	0.600×10^3	0.446×10^3	0.374×10^3	0.280×10^3	50.0
20	2	33.0	0.72	0.021	537.0	4.27	0.157	179.5	0.594×10^3	0.441×10^3	0.370×10^3	0.277×10^3	54.5
21	2	33.0	0.72	0.031	520.0	—	0.157	173.6	0.556×10^3	0.413×10^3	0.346×10^3	0.259×10^3	52.8
22	2	35.3	0.175	0.031	347.0	6.10	0.168	116.8	0.254×10^3	0.189×10^3	0.158×10^3	0.119×10^3	38.7
23	2	35.3	0.36	0.031	392.0	5.96	0.175	131.6	0.324×10^3	0.241×10^3	0.202×10^3	0.151×10^3	45.2
24	2	35.3	0.72	0.012	475.0	2.95	0.163	159.0	0.473×10^3	0.351×10^3	0.295×10^3	0.221×10^3	50.9
25	2	35.3	0.72	0.021	459.0	4.56	0.174	153.9	0.443×10^3	0.329×10^3	0.276×10^3	0.207×10^3	52.6
26	2	35.3	0.72	0.031	448.0	9.75	0.154	149.4	0.419×10^3	0.311×10^3	0.261×10^3	0.195×10^3	45.2
27	2	27.9	0.175	0.031	689.0	9.63	0.156	230.0	0.103×10^4	0.767×10^3	0.643×10^3	0.482×10^3	73.7
28	2	27.9	0.36	0.031	735.0	—	0.147	245.0	0.117×10^4	0.870×10^3	0.730×10^3	0.547×10^3	73.5
29	2	27.9	0.72	0.012	788.0	5.00	0.124	261.0	0.133×10^4	0.991×10^3	0.831×10^3	0.623×10^3	66.5
30	2	27.9	0.72	0.021	759.0	6.95	0.145	251.8	0.124×10^4	0.923×10^3	0.774×10^3	0.580×10^3	75.0
31	2	27.9	0.72	0.031	754.0	10.05	0.161	250.7	0.123×10^4	0.916×10^3	0.768×10^3	0.575×10^3	82.7
32	4	23.6	0.175	0.031	491.0	3.85	0.123	314.4	0.195×10^4	0.145×10^4	0.121×10^4	0.909×10^3	154
33	4	23.6	0.36	0.031	493.0	5.62	0.146	316.4	0.197×10^4	0.147×10^4	0.123×10^4	0.921×10^3	184
34	4	23.6	0.72	0.012	506.0	2.92	0.116	323.2	0.206×10^4	0.153×10^4	0.128×10^4	0.962×10^3	150
35	4	23.6	0.72	0.021	505.0	4.05	0.127	322.8	0.206×10^4	0.153×10^4	0.128×10^4	0.960×10^3	163
36	4	23.6	0.72	0.031	496.0	5.22	0.148	317.9	0.200×10^4	0.124×10^4	0.124×10^4	0.932×10^3	187
37	4	25.2	0.175	0.031	420.0	5.25	0.127	269.1	0.144×10^4	0.107×10^4	0.895×10^3	0.670×10^3	137
38	4	25.2	0.36	0.031	440.0	4.63	0.116	281.1	0.157×10^4	0.117×10^4	0.978×10^3	0.733×10^3	131

TABLE-2 EXPERIMENTAL AND COMPUTED RESULTS

No.	H/D	W/C %	σ_S kg/cm²	σ_D kg/cm²	Fr cps	Accel. g	h	V_p m/sec	Dynamic Elastic Modulus (kg/cm²)				η $\frac{g\cdot sec}{cm^2}$
									Constrained	$\nu=0.30$	$\nu=0.35$	$\nu=0.40$	
39	4	25.2	0.72	0.031	445.0	4.53	0.114	283.7	0.160×10^4	0.119×10^4	0.999×10^3	0.748×10^3	130
40	4	27.3	0.175	0.031	365.0	5.25	0.121	233.7	0.106×10^4	0.784×10^3	0.658×10^3	0.493×10^3	111
41	4	27.3	0.36	0.031	370.0	5.97	0.115	236.5	0.108×10^4	0.804×10^3	0.675×10^3	0.505×10^3	106
42	4	27.3	0.72	0.012	390.0	3.31	0.089	248.5	0.120×10^4	0.888×10^3	0.745×10^3	0.558×10^3	87.2
43	4	27.3	0.72	0.021	401.0	4.46	0.107	255.7	0.127×10^4	0.941×10^3	0.790×10^3	0.591×10^3	107
44	4	27.3	0.72	0.031	401.0	5.73	0.114	255.7	0.127×10^4	0.941×10^3	0.790×10^3	0.592×10^3	114
45	4	30.9	0.175	0.031	283.0	5.22	0.118	182.3	0.620×10^3	0.461×10^3	0.387×10^3	0.289×10^3	81.4
46	4	30.9	0.36	0.031	306.0	—	0.118	196.8	0.724×10^3	0.538×10^3	0.451×10^3	0.338×10^3	87.9
47	4	30.9	0.72	0.031	334.0	—	0.121	214.5	0.862×10^3	0.640×10^3	0.537×10^3	0.402×10^3	98.6
48	4	35.8	0.175	0.031	206.0	4.96	0.112	132.3	0.318×10^3	0.236×10^3	0.198×10^3	0.148×10^3	54.8
49	4	35.8	0.36	0.031	220.0	4.88	0.118	141.0	0.362×10^3	0.269×10^3	0.226×10^3	0.169×10^3	61.1
50	4	35.8	0.72	0.012									
51	4	35.8	0.72	0.021									
52	4	35.8	0.72	0.031	254.0	4.86	0.130	162.3	0.482×10^3	0.358×10^3	0.300×10^3	0.225×10^3	77.7
53	4	37.4	0.175	0.031	201.0	4.82	0.118	128.2	0.302×10^3	0.224×10^3	0.188×10^3	0.141×10^3	56.2
54	4	37.4	0.36	0.031	218.0	5.10	0.119	138.0	0.352×10^3	0.262×10^3	0.219×10^3	0.164×10^3	60.9
55	4	37.4	0.72	0.012	268.0	2.63	0.120	169.4	0.532×10^3	0.395×10^3	0.331×10^3	0.248×10^3	75.0
56	4	37.4	0.72	0.021	257.0	3.47	0.125	162.2	0.489×10^3	0.363×10^3	0.304×10^3	0.228×10^3	74.8
57	4	37.4	0.72	0.031	244.0	4.85	0.128	154.0	0.440×10^3	0.327×10^3	0.274×10^3	0.206×10^3	72.8
58	4	20.4	0.175	0.031	698.0	9.13	0.107	445.8	0.398×10^4	0.296×10^4	0.248×10^4	0.186×10^4	193
59	4	20.4	0.36	0.031	728.0	7.55	0.112	464.8	0.433×10^4	0.322×10^4	0.270×10^4	0.202×10^4	211
60	4	20.4	0.72	0.031	717.0	5.96	0.121	457.9	0.421×10^4	0.313×10^4	0.262×10^4	0.196×10^4	225
61	4	21.7	0.175	0.031	525.0	9.26	0.113	336.1	0.229×10^4	0.170×10^4	0.143×10^4	0.107×10^4	156
62	4	21.2	0.175	0.031	541.0	4.99	0.116	346.4	0.242×10^4	0.180×10^4	0.151×10^4	0.113×10^4	164
63	4	22.1	0.175	0.031	534.0	7.20	0.102	341.4	0.236×10^4	0.176×10^4	0.147×10^4	0.110×10^4	143
64	4	19.1	0.175	0.031	665.0	8.65	0.091	424.4	0.359×10^4	0.266×10^4	0.223×10^4	0.167×10^4	156
65	4	19.1	0.36	0.031	700.0	5.96	0.103	446.9	0.398×10^4	0.296×10^4	0.248×10^4	0.186×10^4	185
66	4	19.1	0.72	0.031	720.0	5.35	0.122	460.7	0.423×10^4	0.314×10^4	0.264×10^4	0.197×10^4	227
67	8	25.4	0.175	0.031	185.0	3.84	0.080	240.9	0.113×10^4	0.843×10^3	0.707×10^3	0.530×10^3	156
68	8	25.4	0.36	0.031	195.0	3.31	0.076	253.6	0.126×10^4	0.935×10^3	0.785×10^3	0.588×10^3	157
69	8	25.4	0.72	0.012	202.0	2.31	0.070	262.5	0.135×10^4	0.100×10^4	0.841×10^3	0.630×10^3	150
70	8	25.4	0.72	0.021	203.0	3.66	0.074	263.8	0.136×10^4	0.101×10^4	0.849×10^3	0.636×10^3	160
71	8	25.4	0.72	0.031	203.0	4.74	0.085	263.7	0.136×10^4	0.101×10^4	0.850×10^3	0.637×10^3	182
72	8	31.4	0.36	0.031	129.0	3.13	0.088	167.2	0.535×10^3	0.397×10^3	0.333×10^3	0.250×10^3	117
73	8	31.4	0.72	0.031	144.0	3.68	0.099	186.6	0.667×10^3	0.495×10^3	0.415×10^3	0.311×10^3	145
74	8	34.4	0.175	0.031	94.0	2.17	0.120	120.4	0.266×10^3	0.198×10^3	0.166×10^3	0.124×10^3	107
75	8	34.4	0.36	0.031	119.0	2.69	0.107	152.0	0.425×10^3	0.316×10^3	0.265×10^3	0.198×10^3	121
76	8	34.4	0.72	0.031	135.0	2.53	0.107	172.1	0.546×10^3	0.406×10^3	0.340×10^3	0.255×10^3	137

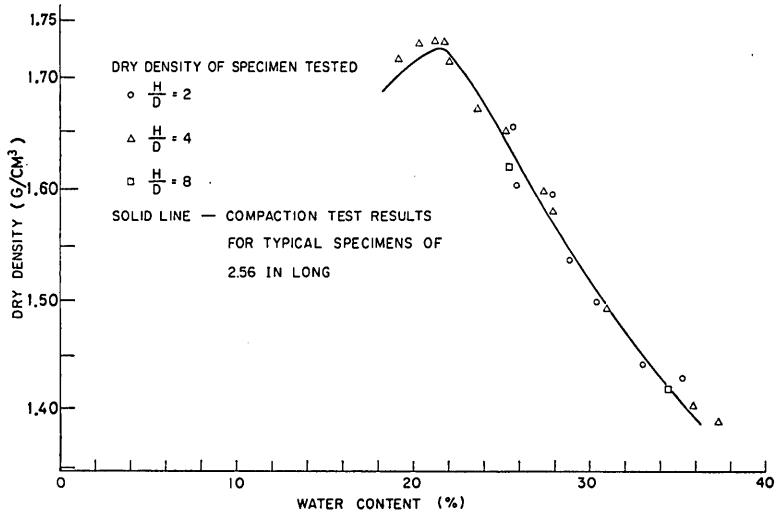

Fig. 13 Dry Density vs Water Content Relation for Tested Specimens

A resonant frequency of the specimen subjected to a vibratory loading is determined as the frequency which corresponds to the peak value of ratio between input and output stresses. Figs. 14 and 15 show the influence of various factors on the relation between resonant frequency and water content.

From these figures it is clearly shown that the water content is an important factor governing the resonant frequency. Although some scatters are observed in the plot,

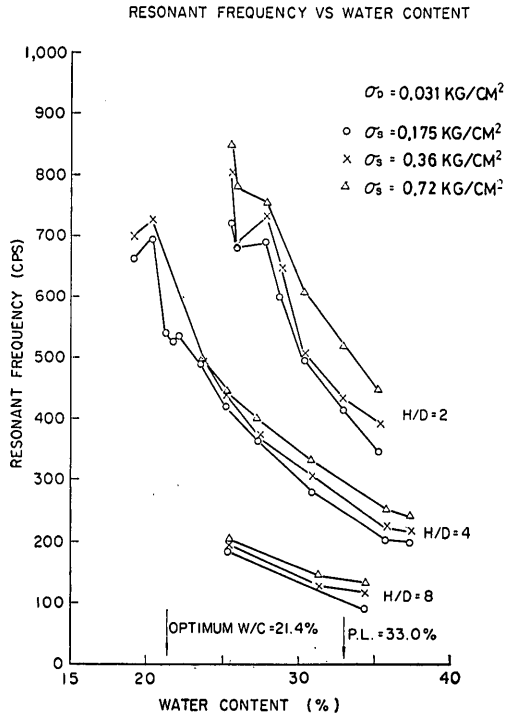

Fig. 14 Resonant Frequency vs Water Content

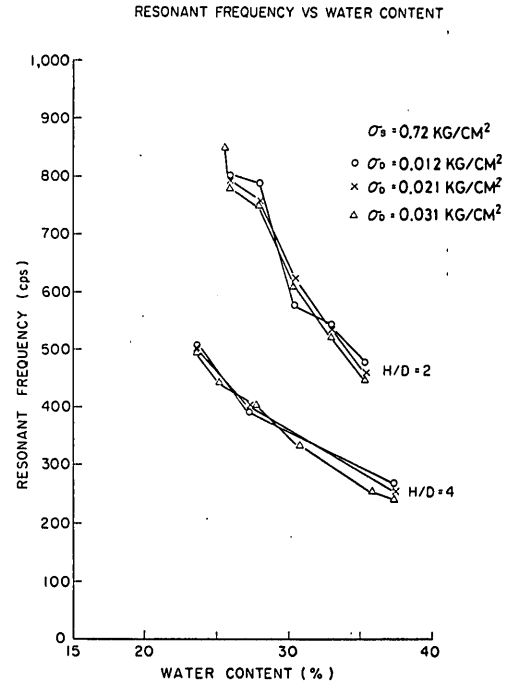

Fig. 15 Resonant Frequency vs Water Content

it may be generally said that the resonant frequency decreases as the water contnent increases.

Stress conditions, in the range used in the present tests, seem to have some influence on the resonant frequency of the specimen. The specimen subjected to the higher static load shows the higher resonant frequency as shown in Fig. 14. As for the dynamic stress level, the higher input stress amplitude seems to give the lower resonant frequency.

6.3 Damping ratio

Determination of the damping ratio defined by Eq. (9) was performed by a best curve fitting procedure as stated previously. The possible variation of damping ratio for various testing conditions will be examined below.

In Fig. 16 is shown an influence of the height-diameter ratio on the variation of damping ratio with water content for different levels of static load. Figs. 17 and 18 show an influence of stress condition on the variation of damping ratio with water content. From these figures, the influence of various factors on values of the damping ratio may be summarised as follows:

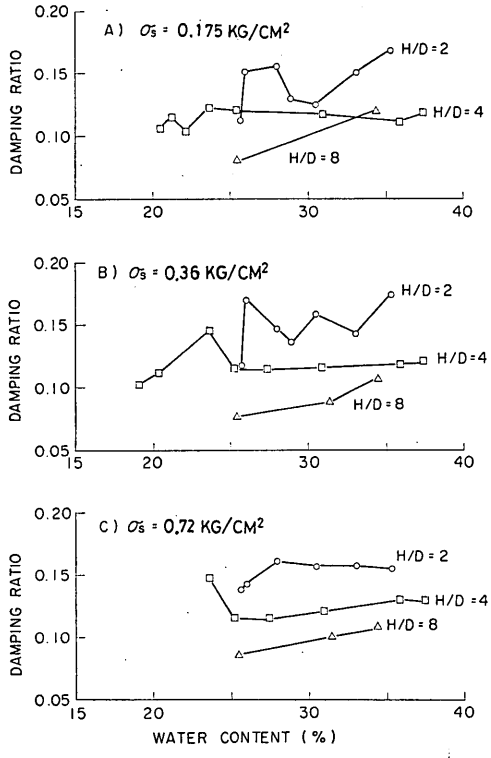

Fig. 16 Damping Ratio vs Water Content

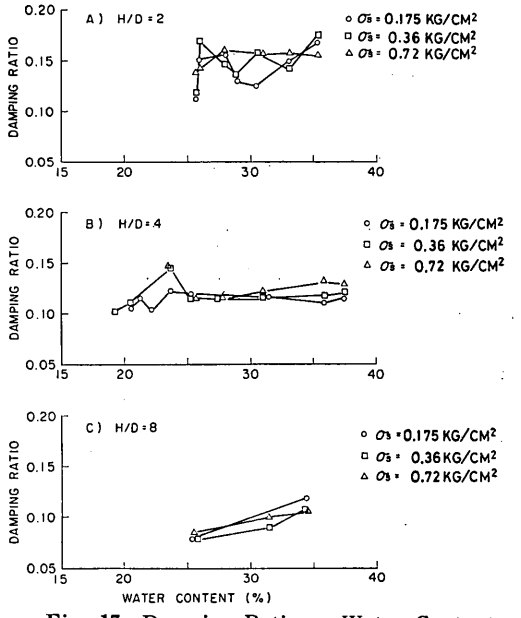

Fig. 17 Damping Ratio vs Water Content

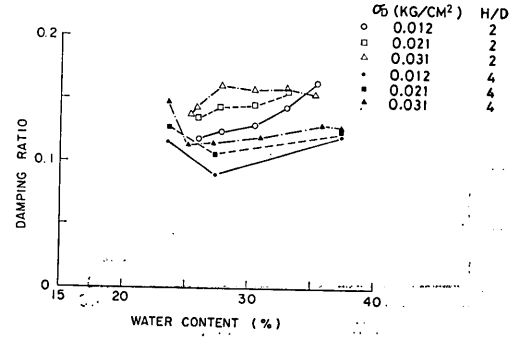

Fig. 18 Damping Ratio vs Water Content (Example for $\sigma_S = 0.72$ kg/cm²)

(1) Water content.....Generally speaking, the damping ratio seems to increase as water content increases. This trend, however, is not so remarkable except the case of $H/D=8$, because of scatters in the data due to other factors such as, presumably, non-uniformity of materials, incomplete constrained conditions at the bottom of the specimen, and so on.

(2) Height-diameter ratio.....It may be generally said from Fig. 16, that the damping ratio increases as the height-diameter ratio decreases, though an opposite tendency is observed at the some water content range because of scatter in the data. If a soil column is composed of the visco-elastic material as represented by the Kelvin model, the damping ratio should be inversely proportional to the height of the specimen, irrespective of other conditions. Quantitative evaluation of influence of height-diameter ratio on viscous parameter is referred to later.

(3) Static stress level.....It seems that the damping ratio is not much affected by the static stress level within the range in the present experiment, although considerable scatters are observed in case of $H/D=2$.

(4) Dynamic stress level.....As shown in Fig. 18, the dynamic stress level seems to have an appreciable influence on the damping ratio. It may be generally said that the higher the dynamic stress level, the higher the damping ratio.

6.4 Longitudinal wave velocity

Longitudinal wave velocities can be obtained by the following theoretical expression

$$V=4Hf_r/\sqrt{1-h^2} \tag{15}$$

where H is height of the specimen, f_r is resonant frequency and h is damping ratio for the fundamental mode.

In Fig. 19, values of longitudinal stress wave velocity obtained from the tests on

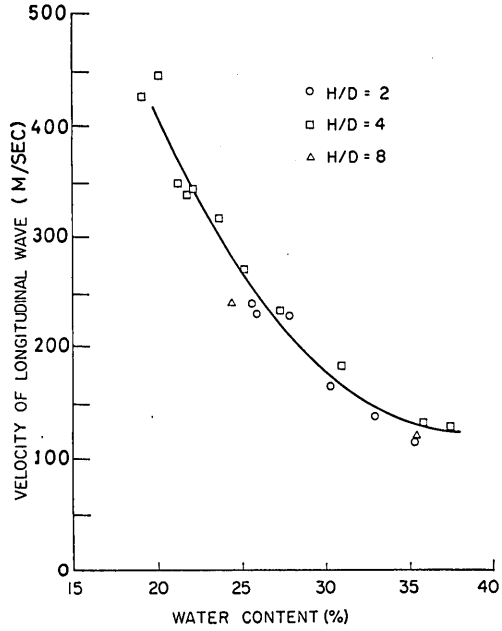

Fig. 19 Relation of V_p and W/C
$\sigma_S=0.175$ kg/cm², $\sigma_D=0.031$ kg/cm²

the specimens having different height are plotted against water content for the case of a static stress level of 0.175 kg/cm². Although a slight scatter is observed in data, it may be said that the wave velocity can be uniquely determined from the resonant column tests on specimens with different height-diameter ratio.

The solid line in Fig. 19 is obtained by the least square method assuming a parabolic curve. Similar curves are for different static stress levels and they are shown in Fig. 20 in order to get a clear picture regarding the influence of static stress level on the variation of longitudinal wave velocities with water content. It will be seen in the figure that the velocity of longitudinal stress wave increases as the static stress level increases. This trend in the wave propagation phenomena is most likely seen in a locking medium, in which the stress-strain curve shows a strain hardnening characteristics.

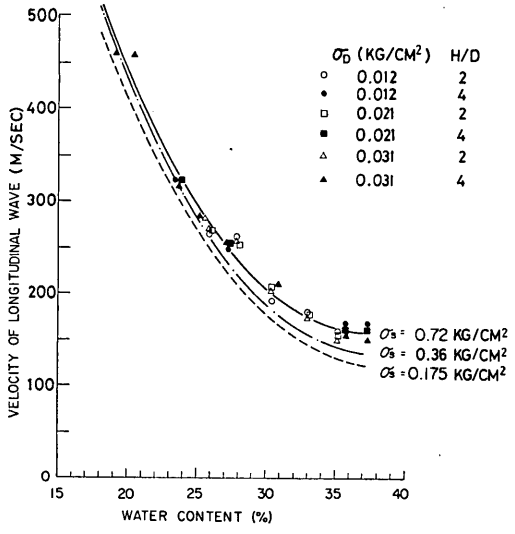

Fig. 20 Relation of V_p and W/C

The influence of input stress amplitude on the variation of longitudinal wave velocities with water content is indicated in Fig. 20 by plotting the data for three different input stresses under a static stress level of 0.72 kg/cm². It appears that the variation of the longitudinal stress wave velocity with water content is not much affected by the input stress amplitudes.

The next factor to be considered is the confining pressure. The theoretical study on the behavior of elastic spheres in contact shows that a longitudinal wave velocity varies with the 1/6 power of the normal stress[23]. Since the soils are greatly apart from the ideal solid, it is necessary to find the wave velocities in real soils by experiments. According to the studies on wave velocities in real soils, it is well known that a confining pressure as well as void ratios is a governing factor to the magnitude of wave velocities in granular soils. These results have been found by means of triaxial apparatuses.

Hardin and Richart[5] investigated the influence of confining pressure on both the longitudinal wave velocity and the shear wave velocity in granular soils under various conditions of density, grain size, gradation and water content. They found that the velocities of both shear and compressive waves for the sands tested varied with appro-

ximately the 1/4 power of confining pressure for high pressures, while for low pressures, the variation was with a power of pressure slightly higher than 1/4. They summarized the experimental results performed by various workers and showed that the velocity of both shear and compressive waves may be a function of confining pressure in the form

$$V=C_1\sigma^{C_2} \tag{16}$$

where C_2 varies in the range of 1/2 to 1/6.

The above mentioned findings are applicable only to granular soils, which are comparatively closer to ideal solids satisfying the conditions considered in the Hertz's contact theory. For cohesive soils, however, much more deviation from ideal solids may be expected. In the author's knowledge, the influence of confining pressure on wave velocities in cohesive soils has not been investigated in detail either experimentally or theoretically, although Hardin and Black[24] got the conclusion that, for normally consolidated clays of low surface activity, the shearing wave velocity may be predicted similarly by the equation in the form of Eq. (16), as long as the shearing strain amplitude is less than 10^{-4}.

Although confining pressures can not be controlled in the present experiment, static stresses initially applied to the specimen work as confining pressures through the lateral confinement due to discrete rings with a small spacing. A value of the confining pressure will be estimated, provided a relevant value of the Poisson's ratio could be assumed.

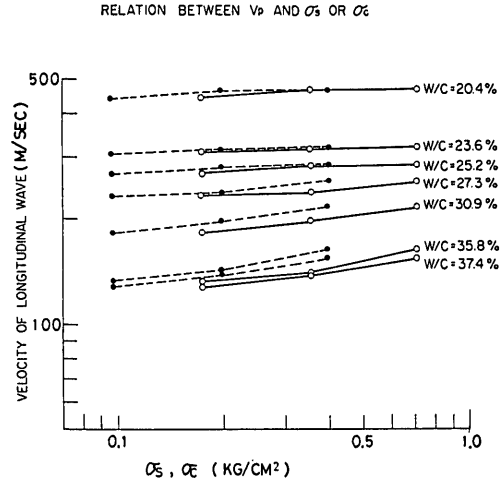

Fig. 21 Relation between V_p and σ_S or σ_C

In Fig. 21, the relation between longitudinal wave velocities and static stress σ_S or estimated confining pressures σ_C for different values of water content is illustrated for the case of $H/D=4$ and $\sigma_D=0.031\,kg/cm^2$. The confining pressure is estimated by assuming a value of Poisson's ratio of 1/3.

Solid lines connecting open circles in Fig. 21 show the relation between longitudinal wave velocity and σ_S, whlist dased lines connecting solid circles show the relation between longitudinal wave velocity and σ_C. Approximately linear relations between wave velocity and σ_S or σ_C on the log-log plot give a C_2 value in Eq. (16) equal to 1/6

for a higher water content range, and this value becomes smaller as water content decreases. Therefore, an influence of static stress on the longitudinal wave velocity depends on the water content, hence the compaction degree of the specimen.

6.5 Visco-elastic parameters

(1) Elastic modulus

The longitudinal wave velocity determined from the specimen height and resonant frequency may be directly associated with the material property such as dynamic elastic modulus in the form of

$$V_p=\sqrt{M/\rho} \tag{17}$$

where M is the related modulus of elasticity and ρ is the density.

In the present experiment, the specimen may be considered to be in a constrained state, thus it is the constained modulus that can be obtained directly from the wave velocity. If the Poisson's ratio is assumed, the Young's modulus can be calculated from the expression

$$E=\frac{(1+\nu)(1-2\nu)}{1-\nu}\cdot E_c \tag{18}$$

where E_c is the constrained modulus of elasticity and ν is the Poisson's ratio.

The variation of elastic modulus E_c with water content of the specimens having different height-diameter ratios is illustrated in Fig. 22, for the case of $\sigma_S=0.175$ kg/cm^2. It is shown that the elastic modulus may be determined independently of height-diameter ratio of the specimen and that it increases as a water content decreases.

In Fig. 22, four solid lines are shown. The uppermost line passing through the plots is determined by the least square method, which shows the variation of constrained modulus of elasticity with water content for a specified stress condition. The variations of Young's modulus computed from the constrained modulus are also shown by the lower three solid lines, which correspond to the Poisson's ratios of 0.3, 0.35 and 0.4 respectively. Since the Poisson's ratio may be expected to vary with water content, the actual variation of Young's modulus with water content may be represented

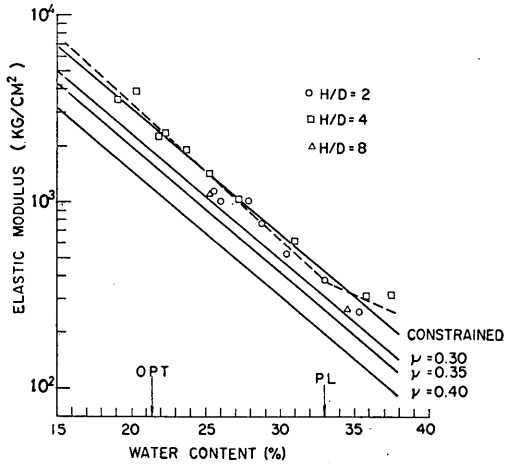

Fig. 22 Dynamic Elastic Modulus vs Water Content
$\sigma_S=0.175$ kg/cm^2, $\sigma_D=0.031$ kg/cm^2

by a line crossing these lines.

In an examination of the relation between elastic modulus and water content, some investigators suggested the importance of the optimum water content or Atterberg's limits (LL and PL).

Wada[25] found that the Young's modulus increased as water content increased up to some value, beyond which the Young's modulus decreased with the increase in water content. And he concluded that it might be the optimum water content at which the variation of elastic modulus with water content changed.

Krizek and Franklin[26] studied the mechanical behavior of a remolded Georgia Kaolin under sinusoidally varying torsional deformations with strain amplitudes up to about 1.5%. They obtained the dynamic complex modulus directly from the stress-time record and examined an influence of water content over a range from 40% to 100%, the liquid limit being 53%. They reported that the complex shear modulus decreased as water content increased, and that the greatest change in the rate of decrease appeared in the vicinity of the liquid limit of the material.

It has been shown that when samples are compacted by kneading action on the wet side of optimum they tend to have a dispersed structure with relatively few strong interparticle contacts, while on the dry side of optimum, samples have flocculated structures with strong interparticle bonds.[27] Therefore, the optimum water content may have a significant bearing on the elastic modulus vs water content curves, since the structure of soils changes remarkably in the either side of the optimum water content[28].

In the present experiment, however, there seems to be no definite evidence that the optimum water content has a special importance in the elastic modulus and water content relation, though only a limitted number of tests have been made in the dry side of the optimum water content.

As for the Atterberg limits of the material used in the present experiment, the plots in Fig. 22 seem to show that the relation between elastic modulus and water content changes somewhere in the vicinity of the plastic limit. It may be interpreted that the constrained elastic modulus rapidly decreases with increase in water content up to the plastic limit, beyond which the rate of decrease in the constrained modulus gradually decreases. Then the variation of constrained modulus with water content may be approximated more reasonably by the dashed line in Fig. 22. The dashed line for the water content below the plastic limit is fitted, for the time being, by the least square method. On the other hand, the dashed line segment for the water content exceeding the plastic limit is drawn by visual judgement.

It should be noted, however, the above mentioned interpretation is acceptable only from practical point of view, since unlike the optimum water content, the Attergerg limits, which are artificially specified, have no physical meaning to cause any change in material properties.

Fig. 23 shows an influence of static stress level on the variation of constrained elastic modulus with water content. Each of two straight lines with a breaking point at the plastic limit was obtained for each level of static stress similarly as described in relation to a dashed line in Fig. 22. Although considerable scatter in the plots, it may be generally said that the constrained modulus for a particular value of water content becomes larger as the static stress level increases. This may be associated with the characteristics of the locking medium as stated previously.

In Fig. 24, the constrained elastic moduli obtained in the vibration under different input stress levels are plotted against the water content for the case of static stress

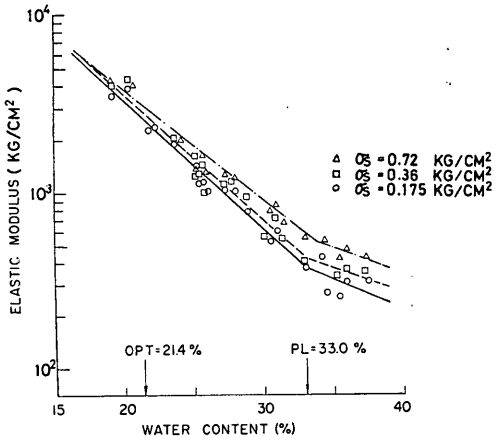

Fig. 23 Dynamic Elastic Modulus vs Water Content

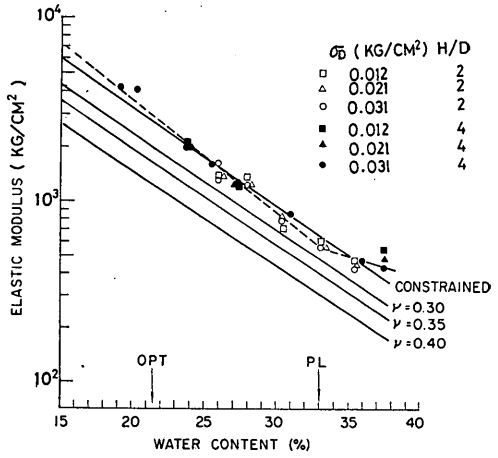

Fig. 24 Dynamic Elastic Modulus vs Water Content (Influence of Input Stress Amplitude for $\sigma_S = 0.72\,kg/cm^2$)

level of 0.72 kg/cm². It will be seen in the figure that the dynamic stress level does not seem to have an appreciable influence on the relation between the constrained elastic modulus and water content. However, a slight tendency may be observed in the range of water content equal to or exceeding the plastic limit, that the higher the dynamic stress level, the lower the modulus. This tendency is more clearly shown in relation to the strain dependency of constrained moduli as referred to later in Fig. 29. This is, however, inconsistent with the typical trend observed in a locking medium. For this point, there seems to be two possible ways in interpreting the experimental data.

One is to regard the stress-strain relation during dynamic loading as actually linear in this limited range of stress levels, and to attridute the minor variation of moduli with an increasing dynamic stress level to the scatter in data.

The other is to attribute such phenomena to non-linear stress strain relation such as S-shaped stress strain curve, with yielding for small stress changes and locking as the stress change is increased further, as shown in Fig. 25. Initial hump is controlled

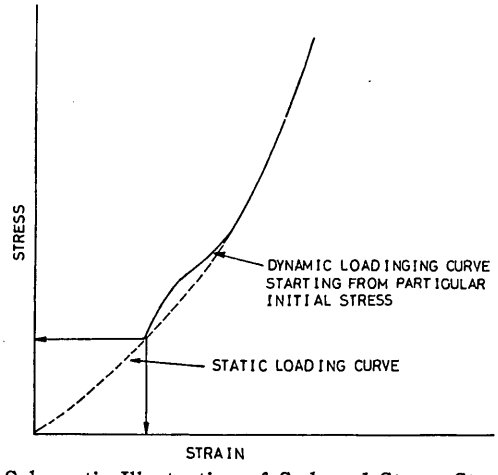

Fig. 25 Schematic Illustration of S-shoped Stress Strain Curve

by the initial static strain and hence by the static stress. The formulation of a hypothesis for S-shaped stress strain relation has been well described by Whitman and Miller[7]. They used this hypothesis to explain the difference between the modulus calculated from the elastic wave velocity and the modulus measured in a compression test.

S-shaped stress strain curves are commonly observed during consolidation testing of clays, where the large stiffness during the early stages of loading is attributed to precompression or to the growth of bonds between particles. Such curves have also been observed during reloading of sand specimens.

Seaman[21] also investigated the wave propagation problem using this concept and established the constitutive relation for static and dynamic loadings in the form

$$\sigma = A\varepsilon^n + B[\varepsilon^{(s)}]^{n_1} \cdot [\varepsilon/\varepsilon^{(s)} - 1]e^{-b[\varepsilon/\varepsilon^{(s)}-1]} \tag{19}$$

where A, B, b are positive constants, ε is total strain and $\varepsilon^{(s)}$ is static strain.

If the hypothesis of S-shaped stress strain relation is applicable to the compacted silty clay sample, the above-mentioned influence of both static and dynamic stress conditions on the elastic modulus could be well explained. To confirm this, it may be necessary to perform the vibratory test under the higher range of dynamic stresses.

(2) Coefficient of viscosity

As for the second parameter of the assumed mechanical model, the coefficient of solid viscosity η may be computed by the expression

$$\eta = 4/\pi \cdot \sqrt{\rho E_c} \cdot hH \tag{20}$$

Figs. 26 and 27 show the variation of coefficient of solid viscosity with water content, in which the computed values of coefficient of solid viscosity are arranged to indicate the influence of testing conditions. From these illustrations, the influences of each factor on coefficient of solid viscosity are summarized as follows:

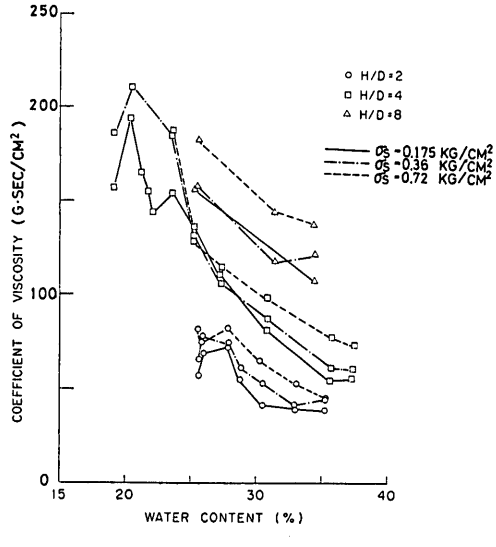

Fig. 26 Relation between η and $W/C(\sigma_D = 0.031\ \mathrm{kg/cm^2})$

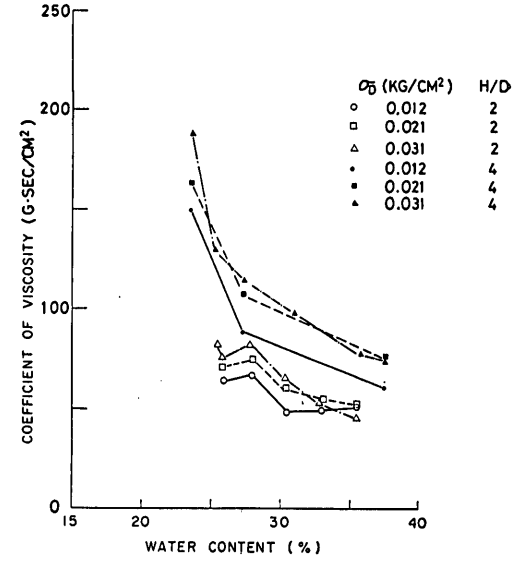

Fig. 27 Relation between η and $W/C(\sigma_S = 0.72\ \mathrm{kg/cm})$

(a) Height-diameter ratio.....The higher the height-diameter ratio, the higher the coefficient of solid viscosity.

(b) Water content.....Generally speaking, the coefficient of solid viscosity decreases as water content increases. In the case of height-diameter ratio of 4, however, a different tendency may be observed at the dry side of the optimum water content, that the peak value of coefficient of solid viscosity seems to appear in the vicinity of the optimum water content.

(3) Estimation of strain

The above mentioned visco-elastic parameters were determined on the basis of the linear visco-elastic model. Since the soil is actually non-linear and non-elastic, the obtained visco-elastic parameters show the stress dependent characteristics even in a very small stress range. Generally, the non-linearity of the materials may be better investigated as strain dependent characteristics rather than as stress dependent characteristics.

In the present test, the input stress whose amplitude is fixed at a specified level causes a different strain because of the difference in compressibility owing to the change in water content. To investigate the strain dependent characteristics of the visco-elastic parameters, the strain amplitude $|\varepsilon_T|$ at the top of the specimen caused by a specified input stress has been estimated by the following expression

$$\varepsilon_T=\left(-\frac{\partial u}{\partial x}\right)_{x=H}=\frac{\sigma_I}{\sqrt{E_c{}^2+p^2\eta^2}}e^{i(pt+\beta)} \tag{21}$$

where σ_I=a specified input stress, E_c=constrained modulus, η=coefficient of solid viscosity and p=circular frequency.

Fig. 28 shows the variation of estimated strain amplitudes at resonance with water content for various input stress levels. The order of estimated strain amplitudes at the top is 10^{-6} to 10^{-4} in the range of the input stress used for the present tests. It may be seen that the higher strain is required to maintain the specified input stress at the top of the specimen for higher water content, and that the logarithm of strain is proportional to the water content.

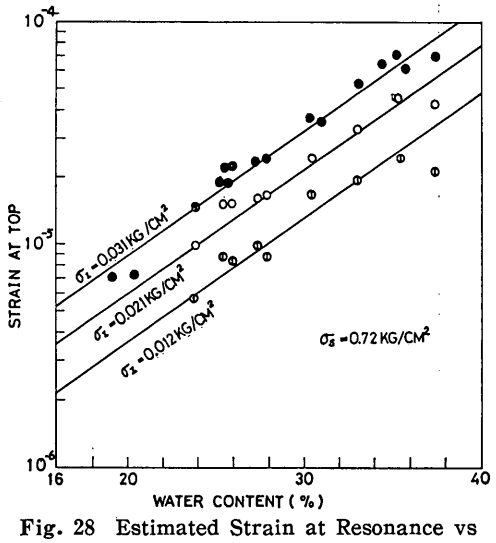

Fig. 28 Estimated Strain at Resonance vs Water Content

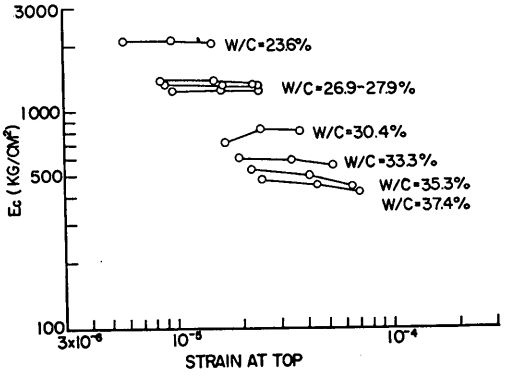

Fig. 29 Strain Dependency of Constrained Modulus of Elasticity

In Fig. 29, constrained moduli are plotted against these estimated strain amplitudes, taking the water content as a parameter. Although the soil is considered to be actually non-elastic and non-linear even in a small strain, it is convenient for practical purposes to define the critical strain within which the soil can be treated as perfectly linear-elastic. It is generally suggested that the critical strain can be considered to be about 10^{-5} to 10^{-4}. From Fig. 29, it may be observed that for lower water content (say less than 30%), a strain required to maintain the specified level of input stress is considered to be within the critical strain, while for higher water content (say more than 30%), constrained moduli tend to show a strain softening characteristics.

7. Discussion

The method of determining the dynamic elastic constants from the resonant frequency of a specimen subjected to a forced vibration was devised in the past. This method has been recognized as a useful tool for a common laboratory procedure, coupled with the recent improvements in testing apparatus and theories for analysis. The originally used resonant column technique has been modified or extended not only for practical use, but also for research. Regarding the technique for predicting dynamic properties from the experimental data obtained in a similar procedure, there are three types of methods available.

The first is the method as adopted by Iida and Ishimoto[3] and others, in which the theoretical relation between height and resonant frequency makes it possible to estimate the wave velocity or solid viscosity coefficient from the experimental data. In this method, all that is required are relative values of amplitudes at frequencies arround resonance. If one wishes to evaluate the effect of frequency on the dynamic properties of soils, however, this method becomes inadequate, as suggested by Kondner[9] and others. Besides this, it is necessary to perform the vibration tests on several specimens of different length in order to determine the dynamic properties of one sample. There is another problem that it is not so easy to fit the theoretical curve to the experimental curve, because of probable scatters in the data, coupled with the fact that it is quite difficult to make several specimens with the same conditions, especially for cohesive soils.

The second is the method in which the elastic parameter and viscous parameter are predicted by fitting the theoretical curve for an assumed physical model to the experimental frequency responses. In principle, only one specimen is required to determine the physical constants for a specified sample.

Yong, et al.[22] discussed the validity of the mathematical predictions based on the Kelvin model. Although recognizing that the correspondence between the actually measured values and those predicted from theory using the analytical model was appreciated, they stressed that it would be dangerous to draw hasty conclusions in predicting wave propagation phenomena based on poorly posed problems and incomplete postulation of boundary conditions, because the pressure wave input is not regular and resonance was not generally encountered in the material in practice.

The third method is the amplitude ratio method, which was originally presented by Lee[29]. In this method, a criterion of amplitude ratio, R, which is the ratio between the displacement at the top and the bottom of the specimen, is used rather than the maximum amplitude as in the case of the resonant column method.

Amplitude ratio is defined in the form

$$R=\left[\sinh^2(\xi k)+\frac{\tan^2(\xi k)}{\tanh^2(\xi k)+\tan^2\theta}\right]^{-\frac{1}{2}} \tag{22}$$

where

ξ=dimensionless frequency factor=pl/V
k=coefficient of damping=tan $\delta/2$
l=length of specimen
V=wave velocity (shear or longitudinal)

By measuring amplitude ratio, R, and phase difference, θ, ξk can be computed, hence wave velocity and coefficient of damping, tan $\delta/2$ can be computed for a known length and given frequency. Although frequency dependency can be easily evaluated in this method, it seems quite difficult to measure the phase difference very accurately.

Elastic parameters and viscous parameters can be obtained by means of either of these three methods. It may be necessary to judge whether the variation of these parameters with variables is based on the change in structures or physical nature of materials, or based on the change in testing conditions. Further, it is necessary to examine the validity of the physical model.

In the analysis of present experimental results, damping ratio, h and wave velocity, V_p were predicted from the frequency responses by the best curve fitting procedures and the variation of these values with variables such as height-diameter ratio, water content, dynamic and static stress levels was investigated. Although only the influence of height, among the variables mentioned above, was considered in the analytical treatment as a visco-elastic column, experimental results show that the influence of height-diameter ratio still appeares in the viscous parameters, as if the material properties of specimen had been changed with its length. This means that the physical model as represented by the Kelvin model is inaccurate in rigorously simulating the vibratory behavior of the soil specimen.

As a consequence of keeping the input stress amplitude constant for varying frequency, an acceleration takes place, depending upon the frequency. The acceleration at the top of the specimen can be computed in terms of the obtained damping ratio. Fig. 30 shows the comparison between computed and measured accelerations (in double amplitude). In the figure, only the variation due to the different height is visualized for different stress conditions. There seems to be a general trend that the computed acceleration corresponding to a damping ratio is higher than the measured acceleration. The discrepancy of measured values from the computed values is greater, especially for the shortest specimen with $H/D=2$. This may be partly due to approximate representation as a Kelvin model. In addition, it may be mainly because of experimental difficulty in controlling the small stress amplitude and partly because of the lateral inertia effect.

In the present studies, experimental data have been presented and discussed to give some information on the dynamic behaviors of soils under one-dimensionlly constrained conditions. To clarify the dynamic behaviour of soils, further theoretical and experimental studies are needed in various aspects, since the soils are far different from the ideal solids. For example, Kondner[9] and Christensen and Wu[30] have conducted the theoretical analyses on the vibratory behaviors of soils using the strain rate dependent dissipative model. Their experiments were in the form of dynamic compression tests on soils. These studies have shown that the dissipative character of certain clay soils is similar to that of the standard linear (3 Element) visco-elastic model in the frequency range considered.

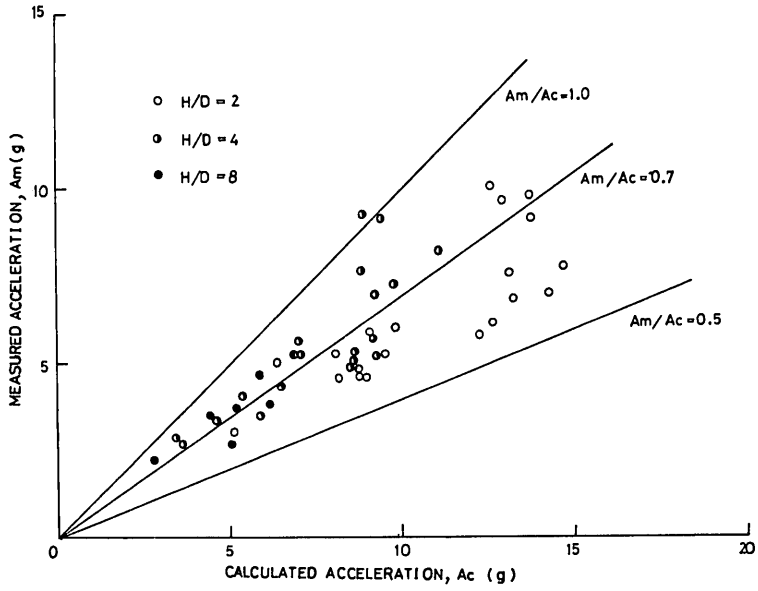

Fig. 30 Measured Acceleration vs Calculated Acceleration

As for the experimental technique adopted, some comparative studies may be needed prior to discussion on the validity of mechanical representation due to a simple Kelvin model. Experimental studies are required on the basis of a force gage concept so that the total force travelling through the soil is measured, in which stress equals the force divided by the cross-sectional area of the column. By using a force gage, one may eliminate the problem of over or under registration which is common with stress gages.

In the present studies, the specimen was alternatively restrained with alumium rings in small spacing. The spacing and weight of aluminum rings may influence evaluated parameters. Effects of these items on the parameters must be investigated on the basis of experimental approach rather than on the basis of theoretical approach, which only makes the problem complicated, because of additional introduction of unknown parameters.

8. Summary and conclusions

A vibrational characteristics of a compacted clay subjected to a longitudinal vibration has been examined by means of the resonant column technique. The specimen was laterally confined with the shells of discrete rings separated by a small spacing, which allowed the vertical motion while preventing the lateral deformation. To avoid the difficulty in the data interpretation associated with the coupling between the driving system and the specimen, stress transducers for measuring both input and output stresses were mounted both on the upper and lower platen in contact with the specimen. The frequency response of base stress to induced top stress was obtained and analysed under the assumption that the soil specimen was composed of visco-elastic materials represented by the Kelvin model. The visco-elastic parameters were obtained by the best curve fitting procedures, and their variation with testing conditions including water

content, height-diameter ratio of the specimen, dynamic stress level and static stress level was investigated. Consequently, the following facts were found:

1. Although the damping ratio is only slightly affected by water content, the damping ratio increases as water content increases. The preload level gives almost no influence on the value of damping ratio, whlist the increase in dynamic stress level gives rise to a slight increase in the damping ratio.

2. The propagation velocity of longitudinal stress wave is obtained independently of height-diameter ratio of the laterally constrained specimen. Hence, the constrained modulus of elasticity and Young's modulus are found to be independent of height-diameter ratio.

3. Both longitudinal wave velocities and elastic parameters are notably influenced by water content and they decrease rapidly as water content increases. The variation of elastic parameters with water content plotted on the semi-log scale seems to be approximated by two straight lines with a breaking point in the vicinity of the plastic limit.

4. The higher preload levels give the higher wave velocities, hence higher elastic parameters. Although these values are not affected so much by the dynamic stress level, there is a tendency that, in the higher range of water content, the elastic parameters and velocities of longitudinal wave decrease as the dynamic stress level increases. These phenomena, which are inconsistent with the general characteristics in static deformation of laterally constrained soil specimens, can be explained only by the S-shaped stress strain relation, unless the minor variations can be attributed to the scatter in the data.

5. The computed value of coefficient of solid viscosity is appreciably affected by each variable of height-diameter ratio, water content, preload level and dynamic stress level. Among them, a considerable influence of height-diameter ratio may suggest that it is actually required to represent the vibratory behavior by means of more complicated mechanical models. However elastic parameters can be determined independently of height-diameter ratio irrespective of the influence of solid viscosity, because the apparent resistance due to solid viscosity seems to be rather small compared with the restoring force in the range of strain used for the present experiment.

Acknowledgements

Experimental works described in this report were conducted at McGill University (Canada) under the financial support by the research grant of Dr, R.N. Yong, whose permission for the use of materials is deeply appreciated. Useful suggestions from Dr. R.D. Japp is also appreciated.

In the course of analysis of the experimental data, the digital computer, TOSBAC 3400, at the Port and Harbour Research Institute was used. (Received Sept. 30, 1972)

References

1) J.W.S. de Graft-Johnson, "The Damping Capacity of Compacted Kaolinite under Low Stresses", Albuqurque, New Mexico, 1967.
2) J.R. Hall and F.E. Richart, "Dissipation of Elastic Wave Energy in Granular Soils", J. Soil Mech. and Found. Div., ASCE, SM6, 1963.
3) M. Ishimoto and K. Iida, "Determination of Elastic Censtants of Soils by means of Vibration Methods, Part 1, Young's Modulus", Bulletin of Earthquake Research Institute, Vol. XIV, 1936, pp. 532–657.

4) M. Ishimoto and K. Iida, "Determination of Elastic Constants of Soils by means of Vibration Methods", Part 2, Modulus of Rigidity and Poisson's Ratio", Bulletin of Earthquake Research Institute, Vol. XV, 1937.
5) B.O. Hardin and F.E. Richart, "Elastic Wave Velocities in Granular Soils", J. Soil Mech. and Found. Div., Proc. ASCE, Vol. 89, No. SM1, Feb., 1963, pp. 33-65.
6) B.O. Hardin and W.L. Black, "Sand Stiffness under Various Triaxial Stresses", J. Soil. Mech. and Found. Div., Proc. ASCE, Vol. 92, No. SM2, March, 1966, pp. 27-42.
7) R.V. Whitman, E.T. Miller and P.J. Moore, "Yielding and Locking of Confined Sand", J. Soil Mech. and Found. Div., Proc. ASCE, Vol. 90, No. SM4, July, 1964, pp. 57-84.
8) H. Kolsky, "Stress Waves in Solids", New York Dover Publications Inc., 1963.
9) R.L. Kondner, "Vibratory Response of A Cohesive Soil in Uniaxial Compression", Second Symposium on Earthquake Engineering, University of Roorkee, India, Nov., 1962, pp. 109-129.
10) G.F. Weissman and R.R. Hart, "The Damping Capacity of Some Granular Soils", Symposium on Soil Dynamics, ASTM, Special Techhical Publication No. 305, 1961.
11) P.W. Taylor and J.M.O. Hughes, "Dynamic Properties of Foundation Subsoils as Determined from Laboratory Tests", 3rd World Conference on Earthquake Engineering, 1965.
12) T. Hatano and H. Watanabe, "Dynamic and Static Visco-elastic Constants and Poisson's Ratio of Clay, Sand and Crushed Stone", Proc. of the Japan Society of Civil Engineers, No. 164, April, 1969, pp. 33-49.
13) C.M. Duke, "Techniques for Field Measurement of Shear Wave Velocity in Soils", 4th World Conference on Earthquake Engineering, Jan., 1969.
14) E. Shima, "Vibration Problems of Subsoil Layers", Proc. Japan Earthquake Symposium, 1966, pp. 437-445.
15) T.Y. Sung, "Vibrations in Semi-Infinite Solids due to Periodic Surface Loadings", Symposium on Dynamic Testing of Soils, ASTM-STP, No. 156, 1953, pp. 35-64.
16) H. Arai and Y. Umehara, "Vibration Characteristics of the Sand Layer", Proc. Japan Earthquake Engineering Symposium, 1966, pp. 73-78.
17) E.T. Selig, "Shock-Induced Stress Wave Propagation in Sand", ph.d. Thesis, Dept. of Civil Engineering, Illinois Institute of Technology, Chicago, Jan., 1964.
18) W. Heierli, "Inelastic Wave Propagation in Soil Columns", J. Soil Mech. and Found. Div., Proc. ASCE, SM6, December, 1962, pp. 33-63.
19) R.D. Stoll and I.A. Ebeido, "Shock Waves in Granular Soil", J. Soil Mech. and Found. Div., ASCE, SM4, 1965.
20) R.D. Stoll and M.S. Hess, "Wave Propagation in A Stress Relaxing Bar", J. Eng. Mech. Div., Proc. ASCE, No. EM5, Oct., 1966, pp. 25-42.
21) L. Seaman, "One-Dimensional Stress Wave Propagation in Soils", Standard Research Institute, DASA 1757, Feb., 1966.
22) R.N. Yong, S.B. Savage and B. Gatehouse, "Wave Propagation and Interaction Effects in Soils", Proc. of the Symposium on Design for Earthquake Loads, McGill University, 1966, pp. V-1-V-35.
23) F.E. Richart, Jr., J.R. Hall, Jr. and R.D. Woods, "Vibration of Soils and Foundations", Prentice-Hall, Inc., Englewood Cliffs, NJ., 1970.
24) B.O. Hardin and W.L. Black, "Vibration Modulus of Normally Consolidated Clay", J. Soil Mech. and Found. Div., Proc. ASCE, Vol. 94, No. SM2, March, 1968, pp. 353-369.

25) T. Wada, "Some Studies on Construction of Earth Dams", Report of the Agricaltural Technology Research Institute, Vol. 1, Tokyo University of Education, 1961.
26) R.J. Krizek and A.G. Franklin, "Non-linear Dynamic Response of soft Clay", Vibration Effects of Earthquakes on Soils and Foundations, ASTM-STP 450, 1968, pp. 96–114.
27) H.B. Seed, J.K. Mitchell and C.K. Chan, "The Strength of Compacted Cohesive Soils, University of Colorado, 1960.
28) T.W. Lambe, "The Structure of Compacted Clay", J. Soil Mech. and Found. Div., ASCE, Vol. 84, No. SM2, 1958.
29) T.M. Lee, "Method of Determining Dynamic Properties of Visco-elastic Solids Employing Forced Vibration", J. of Applied Physics, Vol. 34, 1963.
30) R.W. Christensen and T.H. Wu, "Analysis of Clay Deformation as A Rate Process", J. Soil Mech. and Found. Div., ASCE, Vol. 90, SM6, Nov., 1964.

List of symbols

C =stress amplitude
A, B, b=experimental constants
C_1, C_2=experimental constants
D =diameter
E =Young's modulus
E_c =constrained modulus of elasticity
f_r =resonant frequency
H =height of specimen
h_r =damping ratio of r-order
h =damping ratio of the fundamental mode
i $=(-1)^{1/2}$
k =tan $\delta/2$=coefficient of damping
l =length of specimen
M =related modulus of elasticity
n =undamped natural circular frequency
p =circular frequency of forced vibration
R =amplitude ratio
t| =time
u =displacement
$\ddot{u}$ =acceleration
V =related wave velocity
V_p =longitudinal wave velocity
x =cartesian co-ordinate
W/C =water content
α =acceleration
β =phase difference
ε =axial strain, total strain
$\varepsilon^{(s)}$ =static strain
$\dot{\varepsilon}$ =strain rate
ε_T =strain at top of specimen
ρ =mass density
$\xi = pl/V$=dimensionless frequency factor

η =coefficient of solid viscosity
σ =axial stress
σ_C =confining pressure
σ_D, σ_S =dynamic and static stresses
σ_I, σ_O =input and output stresses
ψ_s =phase difference between input and output stresses
ψ_a =phase difference between input stress and resulting acceleration
ν =Poisson's ratio
δ =phase difference
θ =phase difference

Appendix

If one assumes that the soil column is composed of visco-elastic materials as represented by the Kelvin model having a stress-strain relation in the form

$$\sigma=E_c\varepsilon+\eta\dot{\varepsilon}=E_c\frac{\partial u}{\partial x}+\eta\frac{\partial^2 u}{\partial x\partial t} \tag{1}$$

The basic equation of motion for longitudinal vibration excited one-dimensionally is given by

$$\rho\frac{\partial^2 u}{\partial t^2}=E_c\frac{\partial^2 u}{\partial x^2}+\eta\frac{\partial^3 u}{\partial x^2\partial t} \tag{2}$$

, where ρ: density
E_c: constrained modulus of elasticity
η: coefficient of solid viscosity
u: displacement at x (origin of the x-axis is taken at the bottom of the column)

Putting $u=Ae^{(\iota fx-\omega t)}$ for free vibration, in which the initial and boundary conditions are given by

$$\left.\begin{aligned} &u(x,\,0)=0\\ &u(0,\,t)=0\\ &-\frac{\partial u}{\partial x}=0 \text{ at } x=H \end{aligned}\right\} \tag{3}$$

and substituting into Eq. (2), then the particular solution can be obtained in the form

$$u=Ae^{-\frac{\eta f^2}{2\rho}t}\cos(\omega_r t-\psi)\sin fx \tag{4}$$

$$\omega_r=\sqrt{E_c/\rho\cdot f^2-(\eta f^2/2\rho)^2} \tag{5}$$

, where $f=(2r-1)/2H$ for $r=1, 2, 3,\ldots\ldots$
A=arbitrary constant
ψ=phase difference
ω_r=damped natural circular frequency

The stress at any place in a column is obtained by Eqs. (1) and (4). The stress in a free vibration decreases very rapidly as time lapses.

Next, consider the steady-state forced vibration under the boundary conditions following:

$$u(0,\ t)=0$$
$$\sigma(H,\ t)=Ce^{ipt} \tag{6}$$

, where C is amplitude of input stress and kept constant during vibration, and p is a circular frequency in forced vibration.

Put the particular solution of Eq. (2) in the form

$$u=CD(x)e^{ipt} \tag{7}$$

Put $\lambda=\frac{1\eta}{2\rho}f^2$ and $n^2=\frac{E_c}{\rho}f^2$.

The boundary conditions given in Eq. (6) may be rewritten in the form

$$\left.\begin{aligned} &D=0 \text{ at } x=0 \\ &\frac{dD}{dx}(E+i\eta p)=1 \text{ at } x=H \end{aligned}\right\} \tag{8}$$

Substituting Eq. (7) into Eq. (2) and solving under the boundary conditions in Eq. (8), the stress at the bottom can be given by

$$\sigma(0,\ t)=\frac{C}{\cos(f_1-if_2)H}e^{ipt} \tag{9}$$

, where

$$f_1H=\frac{\pi(2r-1)}{2}\cdot\left(\frac{p}{n}\right)\Big/\left(1+4\left(\frac{p}{n}\right)^2h_r^2\right)^{\frac{1}{4}}\cdot\sqrt{\frac{1}{2}\left(1+1/\sqrt{1+4\left(\frac{p}{n}\right)^2h_r^2}\right)} \tag{10}$$

$$f_2H=\frac{\pi(2r-1)}{2}\cdot\left(\frac{p}{n}\right)\Big/\left(1+4\left(\frac{p}{n}\right)^2h_r^2\right)^{\frac{1}{4}}\cdot\sqrt{\frac{1}{2}\left(1-1/\sqrt{1+4\left(\frac{p}{n}\right)^2h_r^2}\right)} \tag{11}$$

and h_r is a damping ratio and defined by

$$h_r=\frac{\lambda}{n}=(2r-1)\cdot\pi\eta/(4H\sqrt{\rho E_c}) \tag{12}$$

Separating the Eq. (9) into the real and imaginary parts,

$$\begin{aligned}\sigma(0,\ t)&=C/Q\cdot(F_1+iF_2)e^{ipt}\\ &=C/Q\cdot\sqrt{F_1^2+F_2^2}e^{i(pt+\psi_s)}\end{aligned} \tag{13}$$

$$\psi_s=\tan^{-1}F_2/F_1=\tan^{-1}(-\tan f_1H\tanh f_2H) \tag{14}$$

, where
$$\begin{aligned}F_1&=\cos f_1H\cosh f_2H\\ F_2&=-\sin f_1H\sinh f_2H\\ Q&=\frac{1}{2}(\cos 2f_1H+\cosh 2f_2H)\end{aligned} \tag{15}$$

The response of input and output stress is given by

$$\begin{aligned}|\sigma_O|/|\sigma_I|&=1/Q\cdot\sqrt{F_1^2+F_2^2}\\ &=\frac{\sqrt{2}}{\sqrt{\cos 2f_1H+\cosh 2f_2H}}\end{aligned} \tag{16}$$

Differenciating u with t twice, acceleration at the top of the specimen is given in the form

$$\ddot{u}(H, t)=-\frac{C}{\rho H}\cdot\frac{(f_1-if_2)H\cdot\sin(f_1-if_2)H}{\cos(f_1-if_2)H}\cdot e^{ipt} \tag{17}$$

Separating Eq. (17) into the real and imaginary parts, we obtain

$$\ddot{u}(H, t)=\frac{-C}{H\rho Q}\sqrt{(f_1H)^2+(f_2H)^2}\sqrt{\sin^2 2f_1H+\sinh^2 2f_2H}\cdot e^{i(pt+\psi_a)} \tag{18}$$

, which is expressed in the non-dimensional form following

$$\frac{\rho H\ddot{u}}{C}=-\frac{1}{Q}\sqrt{(f_1H)^2+(f_2H)^2}\sqrt{\sin^2 2f_1H+\sinh^2 2f_2H}\cdot e^{i(\dot{p}t+\psi_a)} \tag{19}$$

, where ψ_a is phase difference between induced stress and resulted acceleration and given in the form

$$\psi_a=\tan^{-1}(f_2H\sin 2f_1H+f_1H\sinh 2f_2H)/(f_2H\sinh 2f_2H-f_1H\sin 2f_1H) \tag{20}$$